JOURNAL OF PETROLOGY | VOLUME 47 | NUMBER 12 | PAGES 2463–2489 | 2006 | doi:10.1093/petrology/egl051

Origin and Source Evolution of the Leucite Hills Lamproites: Evidence from Sr–Nd–Pb–O Isotopic Compositions

H. MIRNEJAD[1]* AND K. BELL[2]

[1]GEOLOGICAL SURVEY OF CANADA, 601 BOOTH STREET, OTTAWA, ONTARIO, CANADA K1A 0E8

[2]OTTAWA–CARLETON GEOSCIENCE CENTRE, DEPARTMENT OF EARTH SCIENCES, CARLETON UNIVERSITY, OTTAWA, ONTARIO, CANADA K1S 5B6

RECEIVED JUNE 17, 2003; ACCEPTED AUGUST 21, 2006; ADVANCE ACCESS PUBLICATION SEPTEMBER 20, 2006

Whole-rock major and trace element and O, Sr, Nd and Pb isotopic data are reported for 3·0–0·89 Ma lamproites from the Leucite Hills, Wyoming, USA. The two main groups of lamproites, madupitic lamproites and phlogopite lamproites, are geochemically distinct and cannot be related to one another by either fractional crystallization or crustal contamination. It seems likely that the geochemical differences between these two rock types are related to variations in source mineralogy and depth of partial melting. The high Mg-number and large ion lithophile element abundances and negative ε*Nd values of the lamproites indicate a mantle source that has experienced stages of both depletion and enrichment. The negative Nb, Ta and Ti anomalies in mantle-normalized trace element diagrams and low time-integrated U/Pb, Rb/Sr and Sm/Nd ratios of both lamproite groups and other Cenozoic igneous rocks from the Wyoming Archean Province indicate an ancient metasomatic enrichment (>1·0 Ga) of the mantle source associated with the subduction of carbonate-bearing sediments. Other chemical characteristics of the Leucite Hills lamproites, especially their high K_2O and volatile contents, are attributed to more recent metasomatism (<100 Ma) involving influx from upwelling mantle during back-arc extension or plume activity.*

KEY WORDS: *isotopes; lamproites; metasomatism; Leucite Hills; Wyoming*

INTRODUCTION

Lamproites are Mg-rich igneous rocks (MgO > 5 wt %) that are peralkaline [$(K_2O + Na_2O)/Al_2O_3 > 1$ (molar)], perpotassic [$K_2O/Al_2O_3 > 1$ (molar)] and ultrapotassic [$K_2O/Na_2O > 3$ (molar)]. They span a compositional range of 45–55 wt % SiO_2, 4–10 wt % Al_2O_3, 1–5 wt % TiO_2, 2–10 wt % CaO, 5–10 wt % K_2O, 0·2–1·5 wt % Na_2O and 0·5–2·0 wt % P_2O_5 (Mitchell & Bergman, 1991). Although volumetrically insignificant relative to other potassium-rich igneous rocks, lamproites have attracted a great deal of attention among petrologists because of their unusual geochemistry, distinctive mineralogy and potential to contain diamonds. Lamproites occur in intraplate settings (e.g. USA, Greenland, India, Australia, Antarctica) and in rare instances in post-collisional environments (e.g. SE Spain and central Italy). The Leucite Hills, Wyoming, USA, is considered the type locality for lamproites (Mitchell & Bergman, 1991). Even though the Leucite Hills lamproites (LHL) have been extensively studied for more than a century (e.g. Zirkel, 1867; Cross, 1897; Carmichael, 1967; Fraser, 1987; Mitchell, 1995*a*; Lange *et al.*, 2000), isotope data and trace element concentrations have rarely been reported for the same sample. Considering the distinctive geochemical characteristics of the Leucite Hills lamproites, none of the previous studies have successfully and convincingly explained the nature and the evolutionary history of their mantle sources.

The geochemical characteristics of lamproites, such as high Mg-number and Ni, low Al_2O_3, and very high concentrations of incompatible elements (higher than those of any other alkaline igneous rocks), are consistent with a mantle source that has undergone multiple depletion and enrichment events (Fraser, 1987). The major problem surrounding the petrogenesis of magmas

*Corresponding author. Telephone: (613) 992-4046. Fax: (613) 943-1286. E-mail: hmirneja@nrcan.gc.ca

of lamproitic affinity involves whether their ultimate source is in the lithospheric or sub-lithospheric mantle. Models proposed for the petrogenesis of lamproites range from partial melting of metasomatized lithosphere (e.g. Foley, 1992; Nelson, 1992) to melting of subducted, continentally-derived sediments stored within the Transition Zone at the base of the upper mantle (e.g. Ringwood *et al.*, 1992; Murphy *et al.*, 2002).

In this study, the nature of the mantle source of the LHL is investigated in an attempt to understand the range of chemical (e.g. depletion, enrichment) and geodynamic (e.g. subduction, mantle plume activity) processes that may have contributed to its evolution. This involves a detailed evaluation of the geochemical characteristics of the LHL and integration of data from other Cenozoic volcanic rocks erupted onto the Archean Wyoming craton.

GEOLOGY AND SAMPLE DESCRIPTION

The Leucite Hills are located at 41°47′N, 109°00′W, NE of Rock Springs in Wyoming, USA (Fig. 1). The lamproites in the Leucite Hills cut through the northern flank of the Upper Cretaceous Rock Springs Uplift and clastic sedimentary rocks that belong to the Eocene Fort Union, Wasatch and Green River Formations (Johnston, 1959; Smithson 1959; Bradley, 1964). All of these rocks overlie a thick cratonic basement known as the Wyoming craton. Composed mainly of supracrustal rocks and granitic gneiss terrains, the Wyoming craton experienced multiple episodes of deformation and metamorphism from ~3·0 to 2·5 Ga (e.g. Stuckless *et al.*, 1985; Hofmann, 1989; Frost *et al.*, 1998). Other tectonic events, including folding and faulting, and magmatism also affected the Wyoming craton during the Proterozoic, resulting in a highly fractured, sheared, anisotropic and heterogeneous lithosphere (Blackstone, 1983). Although many of the basement fractures were reactivated during the Phanerozoic, no major deformation of the basement occurred until the late Cretaceous with the onset of the Laramide Orogeny (Blackstone, 1983).

The western United States experienced an abrupt increase in volcanic activity in Eocene to Pleistocene times. In the Wyoming craton, magmatism began around 55 Ma (Absaroka volcanism) and continued until 3·0–0·89 Ma with the eruption of the LHL (Mcdowell, 1971; Mitchell & Bergman, 1991; Lange *et al.*, 2000). The LHL consist of 22 volcanic occurrences that are mostly oriented NW–SE or parallel to structural features such as the Farson Lineament and Maastrichtian thrust fault, which are products of the Laramide Orogeny (Blackstone, 1983; Fig. 1). The lamproites crop out as small groups of volcanic cones, lava flows, plugs and dykes. Highly vesicular scoria and cinders are the dominant materials that make up the tephra cones, whereas flow units and some pyroclastic deposits form composite cones. From field observations, it appears that explosive activity either post-dated or occurred at the same time as the effusive activity.

PETROGRAPHY AND CLASSIFICATION

The petrography of the LHL has been described previously by Cross (1897), Kemp & Knight (1903), Kuehner (1980), Carmichael (1967), Fraser (1987) and Mitchell & Bergman (1991). Therefore, only brief petrographic descriptions of the samples used in this study are given here.

The lamproites that were studied consist mainly of a combination of phlogopite, diopside, sanidine, leucite, apatite, perovskite, and minor K-rich richterite, wadeite, priderite and sherbakovite. Of these minerals, phlogopite, clinopyroxene, and apatite can occur as either phenocrysts or as groundmass crystals, whereas the remainder usually crystallize as groundmass phases. Because lamproites from different parts of the Earth exhibit different and distinct mineralogies and textures, a number of diverse names have been used to classify them. To avoid the use of complicated and unnecessary locality names, the studied samples have been classified using the nomenclature proposed by Scott Smith & Skinner (1984*a*, 1984*b*), Mitchell (1985), Woolley *et al.* (1996) and Le Maitre (2002) (Table 1). As a result, the lamproites from the Leucite Hills can be classified into four groups: (1) diopside–leucite-phlogopite lamproites; (2) diopside–sanidine–phlogopite lamproites; (3) madupitic lamproites; (4) transitional madupitic lamproites. The diopside–leucite–phlogopite lamproites and diopside–sanidine–phlogopite lamproites are genetically related, represent the same magma type (Ogden, 1979; Mitchell & Bergman, 1991), and are collectively referred to as phlogopite lamproites. The madupitic lamproites and transitional madupitic lamproites also show many geochemical affinities (Mirnejad, 2002) and the two are grouped under the heading madupitic lamproites.

ANALYTICAL METHODS

The whole-rock major and trace element compositions of the Leucite Hills samples were measured using inductively coupled plasma (ICP) and ICP–mass spectrometry (MS) facilities, respectively, at Activation Laboratories Ltd., Ancaster, Ontario. Samples were taken into solution using standard fusion techniques. A description of the sample preparation can be found at http://www.actlabs.com. Reproducibility, based on repeat analyses, for the major elements is ±1·0% of the quoted values, whereas most trace elements have an uncertainty of

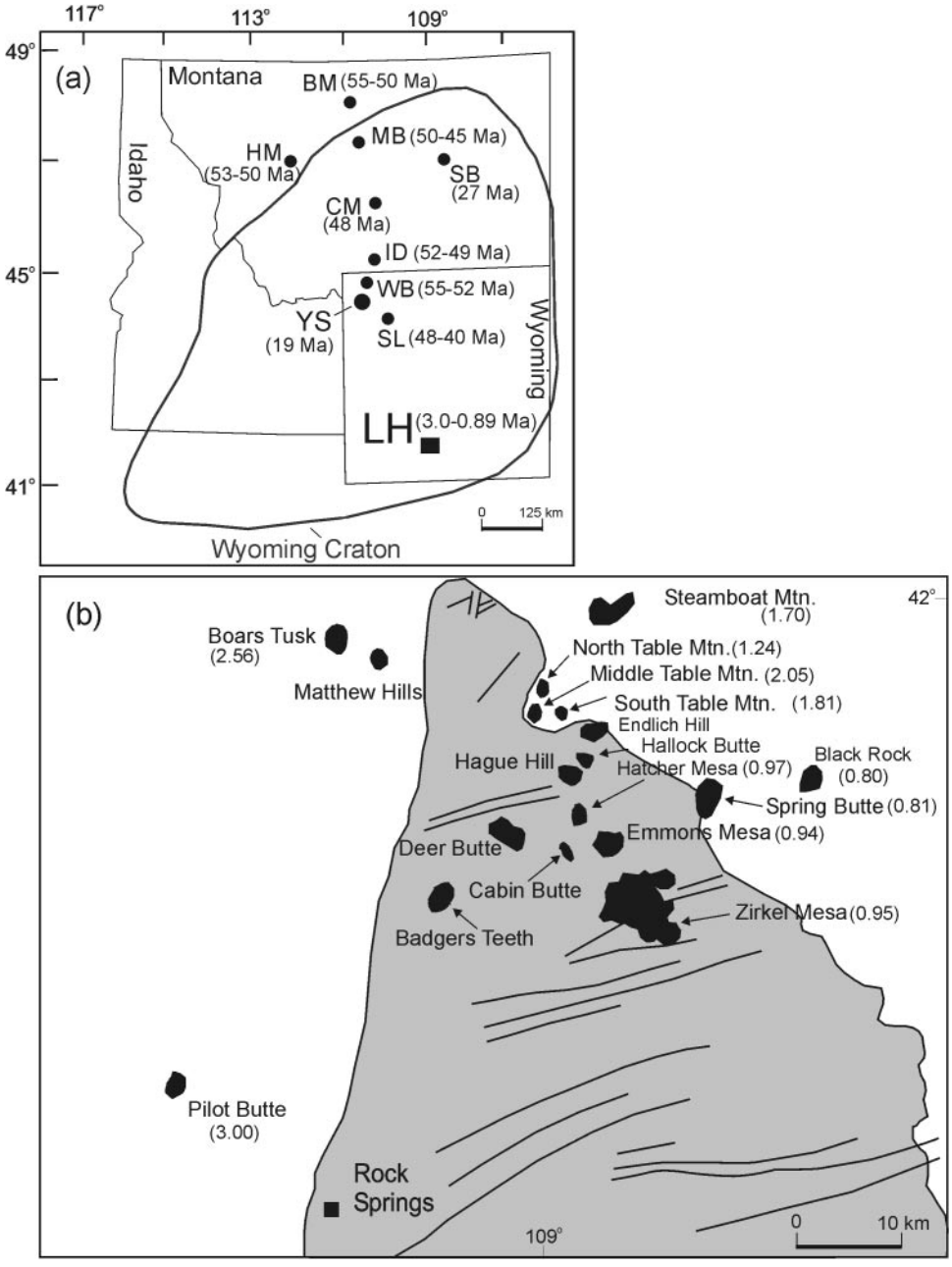

Fig. 1. (a) Map showing the boundary of the Wyoming craton and the location of Cenozoic igneous rocks from the Wyoming Province (after Smith & Braile, 1994; O'Brien *et al.*, 1995). LH, Leucite Hills; SL, Sunlight, Absaroka; WB, Washburn, Absaroka; YS, Yellowstone; ID, Independence; CM, Crazy Mountains; SB, Smoky Butte; MB, Missouri Breaks; HM, Highwood Mountains; BM, Bearpaw Mountains. (b) Map showing location of the LHL (after Mitchell & Bergman, 1991). Numbers in parentheses represent ages in Ma (Lange *et al.*, 2000). Lamproites crop out within Upper Cretaceous sedimentary rocks of the Rock Springs Uplift (shaded area) and Eocene sedimentary rocks of the Fort Union, Wasatch and Green River Formations (white area). The lines on the shaded area mark the positions of Maastrichtian thrust faults.

±5·0% if the concentrations are >100 ppm and ±10% for those with concentrations <100 ppm.

For the radiogenic isotopic analyses, whole-rock powders were digested in Savillex beakers using ultrapure HF and HNO_3 in the proportion 2:5 and were heated for 24 h to ensure complete digestion. Rb, Sr and rare earth elements (REE) were separated from other elements using ion exchange chromatography (Bell & Simonetti, 1996). The procedure is based on HCl elution through 20 cm Teflon columns of 1·0 cm internal diameter filled with 13 ml of Bio-Rad AG50W-X8 cation exchange resin (200–400 mesh). Pb was separated from

Table I: The classification of lamproites and the mineralogy and location of the studied samples from Leucite Hills

Rock type (old terminology)	Orendite	Wyomingite
Rock type (revised terminology)	diopside sanidine leucite phlogopite lamproite	diopside leucite phlogopite lamproite
Principal minerals	Di–Sa–(Lct)–Phl	Di–Lct–Phl
Accessory minerals	Rct–Prd–Wad–Ap	Rct–Prd–Wad–Ap
Locality	North Table Mountain South Table Mountain Zirkel Mesa	Zirkel Mesa

Rock type (old terminology)	Madupite	Transitional madupite
Rock type (revised terminology)	madupitic lamproite	transitional madupitic lamproite
Principal minerals	Phl–Di	Phl–Lct–Di
Accessory minerals	Rct–Prd–Wad–Prv	Rct–Prd–Wad–Prv
Locality	Pilot Butte	Middle Table Mountain Badgers Teeth

The classification of lamproites (after Scott Smith & Skinner, 1984*a*, 1984*b*; Mitchell, 1985; Woolley *et al.*, 1996; Le Maitre, 2002). Abbreviations after Kretz (1983): Ap, apatite; Di, diopside; Phl, phlogopite; Prd, priderite; Prv, perovskite; Rct, richterite; Sa, sanidine; Wad, wadeite; Lct, leucite.

other elements using ion exchange chromatography with HCl, HBr and nanopure H_2O elution through 0·2 and 0·5 ml columns that were filled with AG1-X8 cation exchange resin (100–200 mesh). The average values of total procedural blanks obtained during the study period are as follows: Rb 0·5 ng, Sr 1·5 ng, Sm 0·04 ng, Nd 0·26 ng and Pb 1 ng.

Sr, Nd and Pb isotopic ratios were determined using a Finnigan-MAT 261 multi-collector mass spectrometer at Carleton University operated in the static mode. Samples were loaded on either Ta or Re filaments. A standard was run with every 12 samples. Based on numerous runs during the course of this study, the following average values were obtained for the standards: NBS-987 $^{87}Sr/^{86}Sr = 0{\cdot}710251 \pm 0{\cdot}00003$, La Jolla $^{143}Nd/^{144}Nd = 0{\cdot}511870 \pm 0{\cdot}00003$, NBS-981 $^{206}Pb/^{204}Pb = 16{\cdot}890 \pm 0{\cdot}010$, $^{207}Pb/^{204}Pb = 15{\cdot}429 \pm 0{\cdot}013$, and $^{208}Pb/^{204}Pb = 36{\cdot}498 \pm 0{\cdot}042$. Uncertainties are given at the 2σ level. An average fractionation correction of $0{\cdot}12 \pm 0{\cdot}01\%$ per mass unit was applied to all measured Pb isotopic ratios based on analyses of NBS-981. Measured Sr and Nd isotopic ratios for the unspiked samples were corrected for fractionation to an $^{88}Sr/^{86}Sr$ ratio of 8·3752 and a $^{146}Nd/^{144}Nd$ ratio of 0·7219. Reproducibility for both Nd and Sr isotopic ratios is ±0·004% of the quoted values.

For O isotopic analysis, ~7 mg of the whole-rock sample was oven-dried for 24 h. Samples were then transferred to Ni bombs and fluorinated with BrF_5. The Ni bombs were heated at 600°C for 12 h. Extracted O_2 was converted to CO_2 and then measured on a Finnigan-MAT 252 multi-collector mass spectrometer at the Geological Survey of Canada, Ottawa. The $^{18}O/^{16}O$ ratios of the samples were normalized to an internal standard and then to V-SMOW. The reproducibility of O isotopic ratios based on multiple runs of NCSU-Qtz is ±0·2‰.

CHEMICAL COMPOSITION

Major and trace element analyses of the LHL samples are given in Tables 2 and 3. Additional major and trace element data can be found in papers by Carmichael (1967), Kuehner (1980), Fraser (1987) and Mitchell & Bergman (1991). The major element (wt %) compositions of the LHL based on our new data are: 41·02–55·82 SiO_2, 7·20–9·99 Al_2O_3, 4·13–6·41 Fe_2O_3T, 2·05–2·73 TiO_2, 3·30–12·72 CaO, 4·74–11·54 K_2O, 0·54–1·85 Na_2O and 1·30–2·99 P_2O_5. These values are close to the ranges for lamproites cited by Mitchell & Bergman (1991). The Mg-numbers are all very similar and range from 0·72 to 0·79.

Madupitic lamproites from Pilot Butte and Badgers Teeth have the highest MgO and some of the lowest SiO_2 contents of any of the LHL. The highest P_2O_5 concentrations are shown by the madupitic lamproites from the Badgers Teeth locality. Figure 2 shows the variation of Fe_2O_3T vs SiO_2 (Fig. 2a) and Al_2O_3 vs CaO (Fig. 2b). In both diagrams the LHL show negative correlations and form two distinct groups with the madupitic lamproites having higher Fe_2O_3T and CaO and lower SiO_2 and Al_2O_3 contents than the phlogopite lamproites. For comparison, the compositions of lamproites from Western Australia, Antarctica (Gaussberg), Spain and Italy are also plotted in Fig. 2. The Western Australia and the Gaussberg lamproites have higher Fe_2O_3T contents, whereas most of the lamproites from Italy and Spain have higher Al_2O_3 contents than the LHL.

Trace element concentrations in the LHL are given in Table 3. Ba ranges from 4470 to 11 690 ppm, Sr from 1830 to 7233 ppm, Rb from 166 to 296 ppm, and La from 119 to 402 ppm. As with other lamproites, the Ni (104–333 ppm) and Cr (136–560 ppm) abundances in the LHL are greater than in many other alkaline igneous rocks. The average concentrations of Ta and Nb in the madupitic lamproites are 6 and 125 ppm, respectively, whereas for the phlogopite lamproites they are 3 and 47 ppm, respectively. Madupitic lamproites also have

Table 2: Major element (wt %) composition of the Leucite Hills lamproites

Location:	Badgers Teeth				Pilot Butte			
Rock type:	Madupitic lamproite				Madupitic lamproite			
Sample:	110 BGT	112 BGT	114 BGT	116 BGT	133 PLB	135 PLB	136 PLB	137 PLB
SiO_2	43·2	41·9	42·0	43·9	42·2	41·4	42·4	45·3
TiO_2	2·29	2·19	2·16	2·24	2·28	2·23	2·25	2·05
Al_2O_3	7·85	7·72	8·01	8·36	7·46	7·42	7·20	7·64
MgO	10·5	10·0	10·0	9·3	12·0	12·2	11·2	10·6
CaO	11·1	12·3	10·8	10·0	12·4	12·7	12·4	11·0
Fe_2O_3T	5·94	5·58	5·76	5·69	6·38	6·24	6·16	5·89
MnO	0·10	0·10	0·11	0·09	0·13	0·12	0·12	0·12
Na_2O	1·23	1·06	1·70	0·90	0·55	0·48	0·89	1·67
K_2O	6·85	4·74	6·20	8·14	5·39	5·13	6·59	8·03
P_2O_5	2·92	3·01	2·84	2·99	1·63	1·87	1·83	2·05
LOI	5·42	9·05	6·80	5·86	6·51	6·43	6·98	4·48
Total	97·3	97·6	96·4	97·5	97·0	96·3	98·0	98·9
Mg-no.	0·76	0·76	0·76	0·75	0·77	0·78	0·77	0·76

Location:	Pilot Butte		Middle Table Mt.		South Table Mt.		North Table Mt.	Zirkel Mesa
Rock type:	Madupitic lamproite		Madupitic lamproite		Phlogopite lamproite		Phl lamp	Phl lamp
Sample:	138 PLB	140 PLB	147 MTM	149 MTM	150 STM	151 STM	141 NTM	119 ZM
SiO_2	42·9	43·0	47·4	48·3	53·9	53·1	55·8	55·1
TiO_2	2·26	2·23	2·37	2·55	2·39	2·39	2·58	2·73
Al_2O_3	7·57	7·51	8·66	8·63	9·12	9·07	10·0	9·87
MgO	11·3	10·9	8·87	9·09	9·79	9·72	6·44	6·28
CaO	12·1	12·1	9·34	8·78	4·02	3·86	3·30	4·11
Fe_2O_3T	6·30	6·41	5·45	5·65	4·72	4·61	4·13	0·06
MnO	0·12	0·12	0·09	0·10	0·06	0·06	0·05	4·28
Na_2O	0·54	0·94	1·18	0·96	1·08	1·17	1·69	0·98
K_2O	7·40	8·69	7·29	9·57	11·4	10·5	10·5	11·5
P_2O_5	1·78	2·39	1·30	1·40	1·57	1·35	1·46	1·29
LOI	6·03	4·59	6·79	4·48	2·31	2·31	3·46	3·23
Total	98·3	98·9	98·7	99·5	100·3	98·1	99·4	99·4
Mg-no.	0·76	0·75	0·75	0·74	0·79	0·79	0·74	0·73

Mg-number = $[Mg/(Mg + 0{\cdot}899Fe^{3+})]$. The low total in some samples can be attributed to the high trace element contents. Phl lamp, phlogopite lamproite. LOI, loss on ignition.

higher average Th (45 ppm) and U (10 ppm) contents than the phlogopite lamproites (Th 16 ppm, U 4 ppm). The Sr concentrations of the madupitic lamproites range from 2965 to 7233 ppm, values that are higher than the range found in the phlogopite lamproites (1830–2149 ppm).

One of the characteristic features of the LHL is their high concentration of REE and high light REE/heavy REE (LREE/HREE) ratios [$(La/Yb)_N = 150–600$]. The LREE concentrations and the $(La/Yb)_N$ ratios are shown in Fig. 3a; these are higher in the madupitic lamproites than in the phlogopite lamproites (Fig. 3a, inset). A compilation of REE data from lamproites worldwide (Mitchell & Bergman, 1991) shows that the LHL do not differ greatly from other lamproite types in terms of REE abundance and LREE enrichment.

Trace element data for the LHL normalized to primitive mantle values are plotted on a conventional

Table 3: Trace element (ppm) composition of the Leucite Hills lamproites

Location:	Badgers Teeth				Pilot Butte			
Rock type:	Madupitic lamproite				Madupitic lamproite			
Sample:	110 BGT	112 BGT	114 BGT	116 BGT	133 PLB	135 PLB	136 PLB	137 PLB
V	129	65	116	114	31	21	54	56
Cr	469	489	471	471	546	560	523	444
Co	25	24	27	27	29	30	27	27
Ni	142	148	109	128	120	121	161	104
Cu	38	34	30	28	37	42	54	49
Zn	97	64	72	66	81	74	116	99
Ga	24	23	25	24	23	23	21	24
Ge	1·6	1·6	2·1	2	2·1	2·3	1·9	1·9
As	9	*	*	*	*	*	*	*
Rb	166	226	215	268	177	166	206	212
Sr	6223	5323	5745	5250	7233	6628	4881	5719
Y	23	22	20	20	22	22	25	27
Zr	234	140	634	788	705	793	263	529
Nb	109	98	127	127	139	136	133	136
Mo	*	*	0·4	0·6	0·3	0·3	*	*
Ag	*	1·8	*	*	*	*	*	*
In	*	*	*	0·1	0·1	0·1	*	*
Sn	2	1	3·9	5·2	5·5	3·7	4	5
Sb	0·3	*	0·35	0·35	0·57	0·55	0·6	0·4
Cs	1·7	2·3	5·1	4·6	3·7	3·7	3·1	3·8
Ba	8171	10300	12500	9920	11020	11690	10590	7212
La	397	402	370	395	338	321	371	376
Ce	735	754	739	778	685	653	695	712
Pr	81·5	83·3	81·4	85·6	77·4	73·5	79·5	80·1
Nd	292	300	286	299	276	265	294	300
Sm	33·0	33·8	34·6	35·6	35·7	33·9	35·7	36·0
Eu	7·0	7·0	7·1	7·6	7·7	7·3	7·5	7·7
Gd	20·6	21·5	13·4	13·9	15·9	14·1	22·2	22·7
Tb	1·6	1·6	1·3	1·3	1·5	1·4	1·8	1·8
Dy	5·4	5·1	5·1	5·5	5·8	5·5	5·8	6·1
Ho	0·7	0·7	0·6	0·7	0·7	0·7	0·7	0·8
Er	1·4	1·4	0·7	0·8	0·9	0·8	1·5	1·7
Tm	0·1	0·1	0·1	0·1	0·1	0·1	0·1	0·2
Yb	0·57	0·49	0·43	0·46	0·52	0·46	0·61	0·77
Lu	*	*	0·09	0·10	0·09	0·10	*	*
Hf	4·6	2·4	19	22	10	8·8	1·3	4·7
Ta	5·4	5·3	4·78	4·45	6·23	5·51	6·9	6·7
W	0·7	1·0	0·2	1·4	0·2	0·3	1·6	0·4
Tl	1·20	0·25	1·58	1·46	0·46	0·94	0·15	0·47
Pb	42	31	43	52	53	43	52	120
Bi	0·35	0·22	0·77	1·2	1·27	1·05	0·27	0·31
Th	44·2	43·4	45·9	48	47·4	47·1	42·8	44·8
U	11·4	10·1	10·2	11·4	11	10·7	10·7	10·7

Location:	Pilot Butte		Middle Table Mt.		South Table Mt.		North Table Mt.	Zirkel Mesa
Rock type:	Madupitic lamproite		Phlogopite lamproite		Phlogopite lamproite		Phl lamp	Phl lamp
Sample:	138 PLB	140 PLB	147 MTM	149 MTM	150 STM	151 STM	141 NTM	119 ZM
V	109	69	119	114	86	85	80	90
Cr	541	517	408	415	477	473	310	343
Co	26	26	25	24	28	26	18	21
Ni	155	157	115	156	333	275	180	226
Cu	44	45	28	39	32	22	29	35
Zn	70	68	61	115	96	74	62	67
Ga	20	23	23	25	22	22	23	24
Ge	2·1	1·6	2	1·9	1·5	1·8	1·8	1·9
As	*	6	*	*	*	*	*	*
Rb	258	220	231	302	266	281	296	288
Sr	4126	3814	2965	3051	2132	2149	2020	1830
Y	20	27	16	18	16	15	15·7	12·9
Zr	850	253	808	737	417	588	265	159
Nb	123	123	97	104	47	46	39·6	41·9
Mo	0·8	*	0·3	*	*	0·8	*	*
Ag	*	*	*	*	*	*	*	*
In	*	*	*	*	*	*	*	*
Sn	3·3	3	3·9	5	5	4·1	6	5
Sb	0·49	0·4	0·41	0·3	0·2	0·27	0·4	0·6
Cs	4·1	2·9	2·9	3·1	2·0	2·5	1·8	2·2
Ba	7556	9087	8453	6451	4471	4777	6670	6240
La	373	351	271	262	140	133	150	119
Ce	740	664	546	504	271	269	297	236
Pr	74·9	75·0	55·2	56·3	31·1	31·1	36·1	27·5
Nd	273	280	200	208	118	112	124	96·8
Sm	34·9	33·8	24·9	24·1	15·0	15·4	15·6	12·8
Eu	6·6	7·1	4·6	5·1	3·3	3·5	3·5	2·7
Gd	16·5	20·7	12·1	14·5	9·86	7·5	9·92	8·02
Tb	2·1	1·7	1·5	1·2	0·9	0·8	0·9	0·7
Dy	5·9	5·9	4·2	4·1	3·5	3·5	3·5	3·0
Ho	0·7	0·8	0·6	0·6	0·5	0·5	0·6	0·5
Er	0·8	1·7	0·7	1·2	1·1	0·8	1·1	0·9
Tm	0·1	0·2	0·1	0·1	0·1	0·1	0·1	0·1
Yb	0·4	0·82	0·37	0·60	0·59	0·52	0·37	0·37
Lu	0·11	*	0·09	*	0·06	0·09	0·03	0·04
Hf	20	1·3	12	8·1	3·3	3	2·5	1·4
Ta	8·81	6·5	6·76	4·9	2·0	2·22	2·4	2·6
W	1·7	0·3	1·6	0·5	1·1	0·9	*	0·7
Tl	1·24	0·39	0·46	0·74	0·85	1·01	0·29	0·54
Pb	52	26	80	47	23	29	25	32
Bi	1·97	0·44	0·83	0·38	0·18	0·68	0·1	0·19
Th	43·2	42·0	34·4	33·5	15·5	16·4	16·7	13·7
U	9·74	8·13	7·38	7·07	5·05	4·85	3·4	3·78

*Below detection limit.
Phl lamp, phlogopite lamproite.

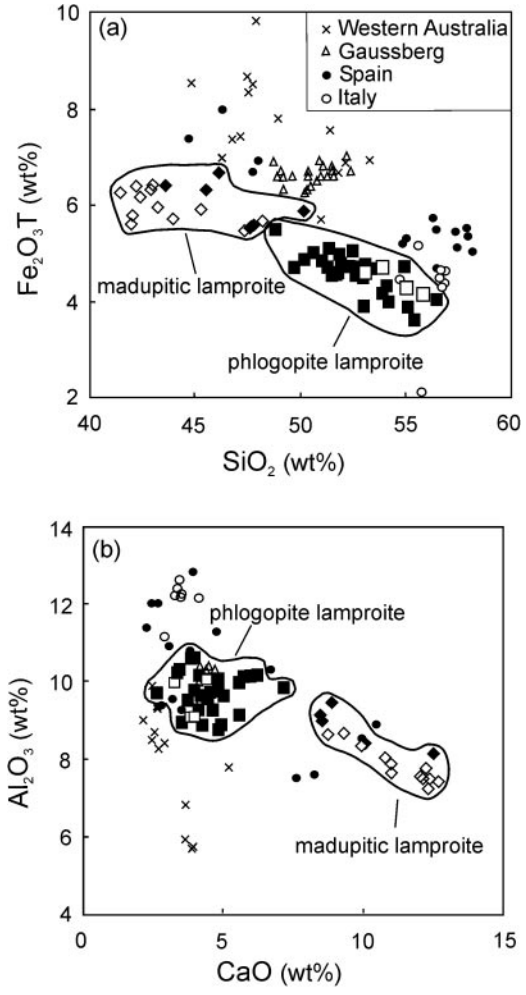

Fig. 2. Variation of Fe_2O_3T vs SiO_2 (a) and Al_2O_3 vs CaO (b) for the LHL. Data sources: this study (filled squares and diamonds), and Carmichael (1967), Vollmer *et al.* (1984), Fraser (1987), and Mitchell & Bergman (1991) (open diamonds and squares). Also shown for comparison are data for lamproites from Gaussberg (Murphy *et al.*, 2002), Spain (Nixon *et al.*, 1984), Italy (Peccerillo & Lustrino, 2005) and Western Australia (Fraser, 1987).

mantle-normalized trace element diagram (Fig. 3b) in order of increasing compatibility from left to right. In general, the madupitic lamproites are more enriched in the large ion lithophile elements (LILE) and high field strength elements (HFSE) than the phlogopite lamproites. The normalized trace element patterns for the various lamproite types show similar enrichments in many of the incompatible trace elements as well as pronounced Nb, Ta and Ti troughs (Fig. 3b).

The combined trace and major element data show that the two groups of the LHL are chemically distinct from one another. Trace element ratios are also distinctive for the phlogopite and madupitic lamproites, including Ba/La, Ba/Th, Ba/Nb, Rb/Nb, Nb/U, Ce/Pb, and Tb/Yb ratios (not shown). The Ce/Pb ratios in the LHL are variable and range from 7 to 25 (average 14), values that almost extend from near the average value of four for the continental crust to 25 for the mantle (Hofmann, 1997).

The whole-rock Sr, Nd and Pb isotopic compositions of the lamproites from this study are listed in Table 4 and plotted in Figs 4 and 5. The Nd–Sr isotopic compositions of the LHL all lie in the enriched quadrant (Fig. 4) and define two groups, one corresponding to the phlogopite lamproites and the other to the madupitic lamproites. From Table 4 and Fig. 4 it can be seen that the madupitic lamproites have higher $^{143}Nd/^{144}Nd$ ratios (0·51203–0·51211, εNd −11·7 to −10·1) than the phlogopite lamproites (0·51186–0·51194, εNd −15·0 to −13·5). $^{87}Sr/^{86}Sr$ ranges from 0·70534–0·70563 for the madupitic lamproites to 0·70566–0·70606 for the phlogopite lamproites. The LHL form a vertical array at relatively constant $^{87}Sr/^{86}Sr$ and variable $^{143}Nd/^{144}Nd$ ratios. Although the LHL have similar εNd values to lamproites from Gaussberg, Spain, Italy and West Kimberley, their $^{87}Sr/^{86}Sr$ ratios are lower.

The madupitic lamproites have Pb isotopic ratios ($^{206}Pb/^{204}Pb$ 17·4–17·58, $^{207}Pb/^{204}Pb$ 15·47–15·50, $^{208}Pb/^{204}Pb$ 37·42–37·52) somewhat higher than those of the phlogopite lamproites ($^{206}Pb/^{204}Pb$ 17·13–17·23, $^{207}Pb/^{204}Pb$ 15·46–15·48, $^{208}Pb/^{204}Pb$ 37·20–37·32) (Fig. 5). Unlike the Pb data from the LHL, those from Western Australia, Gaussberg, Spain and Italy plot above the Stacey–Kramers growth line on the $^{207}Pb/^{204}Pb$ vs $^{206}Pb/^{204}Pb$ diagram (Fig. 5a). Data for all of these lamproites plot above the Northern Hemisphere Reference Line (NHRL).

Some new oxygen isotopic data from the LHL are given in Table 4. The $\delta^{18}O_{SMOW}$ of the samples fall within a relatively narrow range from +8·21 to +8·90‰, and no significant differences are observed between the madupitic lamproites and phlogopite lamproites from different locations.

THE RELATIONSHIP BETWEEN PHLOGOPITE LAMPROITES AND MADUPITIC LAMPROITES

The observation that the LHL form two distinct geochemical groups in most of the major and trace element and radiogenic isotope diagrams means that the madupitic and phlogopite lamproites cannot simply be related by fractional crystallization. Alternative explanations might involve crustal assimilation, variation in depth of partial melting and/or source mineralogy.

Crustal contamination

Although crustal contamination has a minimal effect on the chemical composition of lamproites because of their

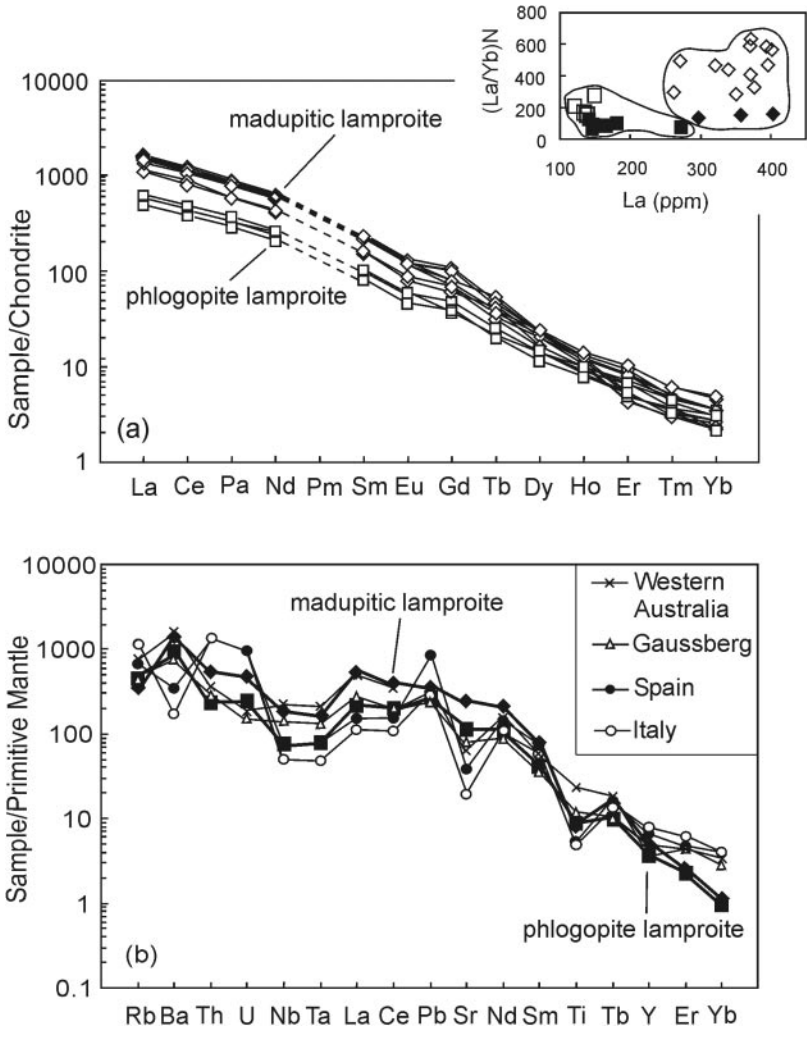

Fig. 3. (a) Chondrite-normalized REE patterns for the LHL. Inset shows normalized La/Yb ratio vs La concentration. (b) Extended trace element patterns of the LHL normalized to primitive mantle values (McDonough & Sun, 1995). The normalized trace element patterns of other lamproites worldwide (average values) show similar trends to those of the LHL. Data sources: madupitic and phlogopite lamproites—this paper; Gaussberg lamproites—Murphy *et al.* (2002); Spanish lamproites—Turner *et al.* (1999); Italian lamproites—Peccerillo & Lustrino, 2005; Western Australian lamproites—Mitchell & Bergman (1991). Symbols as in Fig. 2.

extreme enrichment in incompatible elements as well as their high Ni and Cr contents (Carmichael, 1967; Kuehner, 1980; Vollmer *et al.*, 1984), Ogden (1979) suggested that the madupitic lamproites from Pilot Butte might have attained their distinctive mineralogy and chemical composition by reaction between a phlogopite lamproite melt and entrained crustal rocks, a hypothesis solely based on petrographic and field observations. We tested this using a simple binary mixing model.

Contamination can occur in two ways, one involving mixing between crustal- and mantle-derived melts, and the other by assimilation of crustal rocks. Here, the bulk assimilation model is evaluated using simple binary mixing between upper crustal rocks and lamproite melts. Although a more realistic approach involves the assimilation–fractional crystallization (AFC) model as formulated by DePaolo (1981), the overall outcome is very model dependent, involving such parameters as the composition of the initial magma, the composition of the host rock, the composition of the fractionating phases, the partition coefficients between the fractionating phases and the residual melt, and the rate of assimilation and crystallization (DePaolo, 1981). Because of the lack of constraints on many of these parameters only a bulk assimilation model is considered here.

Wedepohl's (1995) estimate of the composition of the upper continental crust was used as an end-member in the binary mixing calculations. Figure 6a shows that bulk assimilation by the phlogopite lamproites of upper crust increases the Al_2O_3, MnO, and Na_2O abundances

Table 4: The measured Sr, Nd, Pb and O isotopic composition of the Leucite Hills lamproites

Sample	Location	Lamproite type	$^{87}Sr/^{86}Sr$	$^{143}Nd/^{144}Nd$	$^{206}Pb/^{204}Pb$	$^{207}Pb/^{204}Pb$	$^{208}Pb/^{204}Pb$	$\delta^{18}O$ (‰)
110BGT	Badgers Teeth	Madupitic	0·70545	0·51203	17·457	15·484	37·272	8·32
112BGT	Badgers Teeth	Madupitic	0·70538	0·51197	17·446	15·484	37·463	
113BGT	Badgers Teeth	Madupitic	0·70534	0·51203	17·436	15·473	37·424	8·21
114BGT	Badgers Teeth	Madupitic	0·70551	0·51204	17·442	15·481	37·459	8·37
116BGT	Badgers Teeth	Madupitic	0·70537	0·51201	17·444	15·484	37·455	
147MTM	Middle Table Mt.	Madupitic	0·70551	0·51209	17·534	15·491	37·501	8·80
149MTM	Middle Table Mt.	Madupitic	0·70551	0·51206	17·535	15·496	37·512	8·86
133PLB	Pilot Butte	Madupitic	0·70549	0·51210	17·556	15·508	37·489	
135PLB	Pilot Butte	Madupitic	0·70551	0·51209	17·542	15·489	37·480	8·66
136PLB	Pilot Butte	Madupitic	0·70545	0·51209	17·547	15·496	37·517	
138PLB	Pilot Butte	Madupitic	0·70556	0·51211	17·563	15·490	37·485	8·93
140PLB	Pilot Butte	Madupitic	0·70563	0·51208	17·583	15·504	37·523	
119ZM	Zirkel Mesa	Phlogopite	0·70574	0·51187	17·227	15·464	37·318	8·65
120ZM	Zirkel Mesa	Phlogopite	0·70566	0·51191	17·182	15·462	37·258	
122ZM	Zirkel Mesa	Phlogopite	0·70568	0·51194	17·220	15·467	37·320	8·72
141NTM	North Table Mt.	Phlogopite	0·70591	0·51188	17·273	15·482	37·280	8·38
143NTM	North Table Mt.	Phlogopite	0·70603	0·51186	17·281	15·482	37·278	
144NTM	North Table Mt.	Phlogopite	0·70606	0·51189	17·282	15·478	37·203	8·81
146NTM	North Table Mt.	Phlogopite	0·70603	0·51187	17·239	15·470	37·239	
150STM	South Table Mt.	Phlogopite	0·70585	0·51178	17·227	15·470	37·159	8·58
151STM	South Table Mt.	Phlogopite	0·70584	0·51183	17·254	15·477	37·188	
152STM	South Table Mt.	Phlogopite	0·70608	0·51178	17·250	15·460	37·130	8·74
153STM	South Table Mt.	Phlogopite	0·70592	0·51181	17·253	15·459	37·170	8·68
154STM	South Table Mt.	Phlogopite	0·70595	0·51181	17·247	15·466	37·158	8·52

Uncertainties are given at 2σ level. The reproducibility of Pb isotopic ratios is 0·1% at the 2σ level. Because the Leucite Hill Lamproites are young (3·0–0·89 Ma), the initial and measured isotopic ratios are similar within analytical uncertainty.

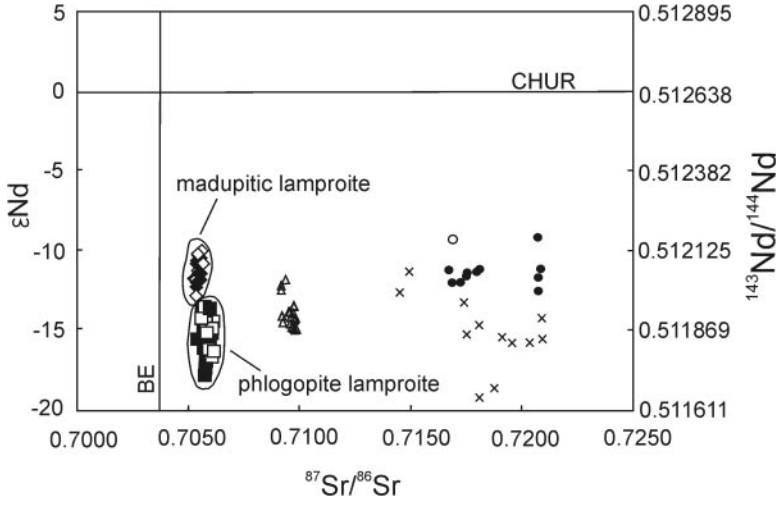

Fig. 4. εNd vs $^{87}Sr/^{86}Sr$ for the lamproites from Leucite Hills, Gaussberg, Spain, Italy and West Kimberley. Data sources as in Fig. 3 and symbols as in Fig. 2. BE, Bulk Earth; CHUR, Chondritic Uniform Reservoir.

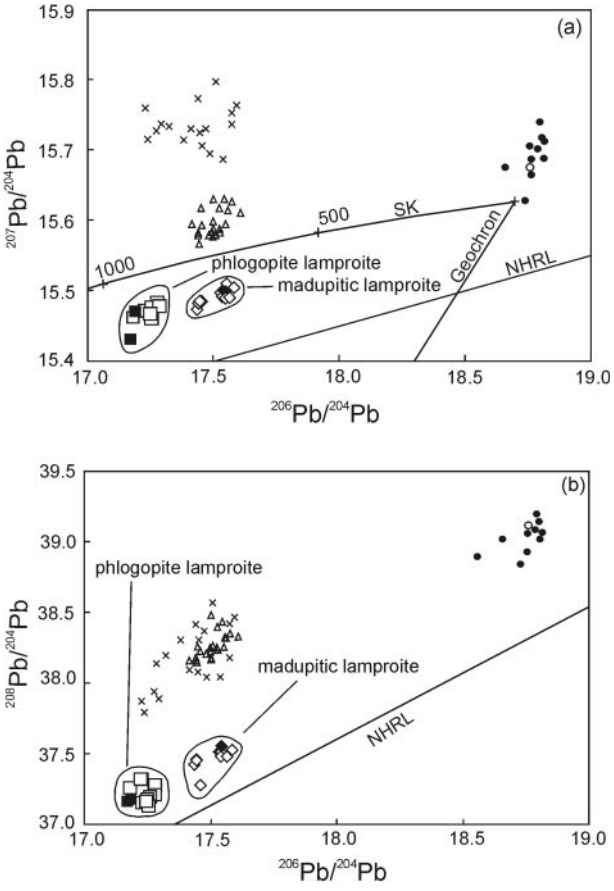

Fig. 5. Variation of $^{207}Pb/^{204}Pb$ vs $^{206}Pb/^{204}Pb$ (a) and $^{208}Pb/^{204}Pb$ vs $^{206}Pb/^{204}Pb$ (b). Data sources as in Fig. 3 and symbols as in Fig. 2. SK, Stacey–Kramers growth line (Stacey & Kramers, 1975). Numbers on the growth line indicate time in Ma. NHRL, Northern Hemisphere Reference Line (Hart, 1984).

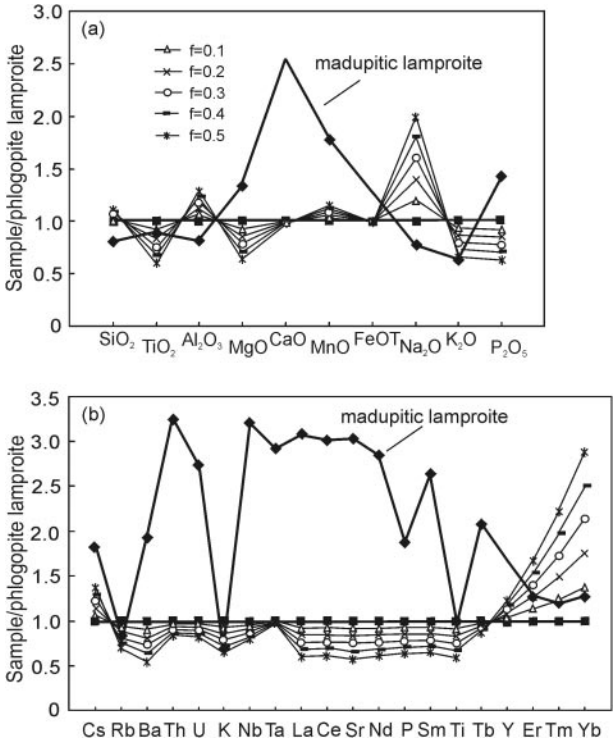

Fig. 6. (a) Major element enrichment or depletion generated by bulk assimilation of upper crust by phlogopite lamproite melt. Data normalized to an average phlogopite lamproite. (b) Trace element enrichment or depletion generated by bulk assimilation of upper crust by phlogopite lamproite melt. Data normalized to average phlogopite lamproite. Shown for comparison are normalized data for a typical madupitic lamproite. f is the weight fraction of the contaminant.

and decreases the TiO_2, MgO, K_2O and P_2O_5 contents of the contaminated magma. In this case, the major element composition of the contaminated phlogopite lamproite magma fails to approach the chemical composition of any of the existing madupitic lamproite types in the Leucite Hills for up to 50% contamination ($f = 0{\cdot}5$, where f is the weight fraction and is calculated as $f = A/(A + B)$; A and B are the weight fractions of the contaminant and the original magma, respectively). Similarly, bulk assimilation of upper crust by the madupitic lamproites cannot generate lamproite melts whose major element contents resemble those of the phlogopite lamproites.

The trace element concentrations of the contaminated magmas, normalized to the average trace element concentration of the phlogopite lamproites, are plotted in Fig. 6b. Contamination by upper crust decreases the concentration of most incompatible elements and increases the concentration of the HREE in the melt. The incompatible element characteristics of the resulting contaminated phlogopite lamproite melt differ significantly from those of the madupitic lamproites. A similar approach shows that contamination of a madupitic lamproite melt by upper crust cannot generate magmas with trace element contents similar to those of the phlogopite lamproites.

The Sr–Nd isotopic data place additional constraints on crustal assimilation models. Contamination by upper crust (Fig. 7a) increases the $^{87}Sr/^{86}Sr$ ratios of the madupitic lamproites to values comparable with those of the phlogopite lamproites but only for $f > 0{\cdot}5$ (i.e. assimilation of >50% of crustal material). The Mg-number and Ni contents of the madupitic lamproites are much too high to allow for such degrees of assimilation. Similarly, the madupitic lamproite melt needs to assimilate substantial amounts of upper crustal rocks ($f > 0{\cdot}5$) for its $^{143}Nd/^{144}Nd$ ratio to reach values close to of those of the phlogopite lamproites (0·5118) (Fig. 7b). However, even though contamination of the madupitic lamproite could generate a melt with a Nd isotopic composition similar to that of the phlogopite lamproites, the major and trace element composition of such a melt are still very different. Assimilation of upper

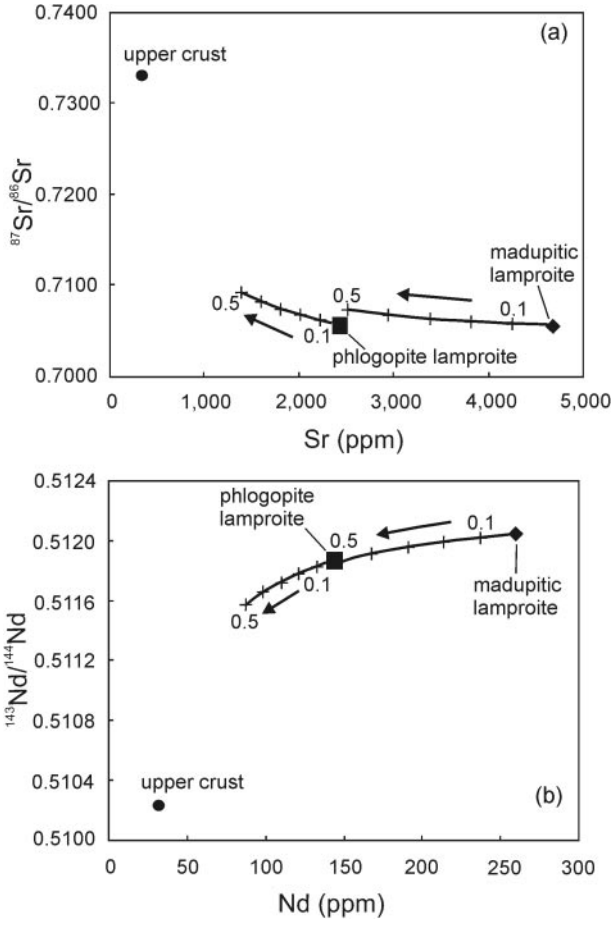

Fig. 7. Upper crustal contamination models. (a) $^{87}Sr/^{86}Sr$ vs Sr (ppm); (b) $^{143}Nd/^{144}Nd$ vs Nd (ppm). Contamination of madupitic lamproite melt by upper crust generates contaminated melts with Nd and Sr isotopic ratios and concentrations similar to those of the phlogopite lamproites but at prohibitively high fractions of contaminant (>50%). Progressive contamination of the phlogopitic lamproite melt by upper crust generates melts whose Nd and Sr isotopic ratios are lower and higher, respectively, than those of the madupitic lamproites. Numbers indicate the weight fraction of the contaminant.

crust by a melt with the composition of a phlogopite lamproite cannot generate a melt with Nd isotopic ratios similar to the madupitic lamproite (Fig. 7b).

On the basis of these simple mixing models, it is unlikely that the two major lamproite types found in the Leucite Hills (i.e. phlogopite lamproite and madupitic lamproite) are related to one another, either by fractional crystallization or by crustal contamination. It is more likely that the geochemical distinctions of these two lamproites represent source variations.

Source mineralogy and depth of partial melting

One explanation for variations in the chemical compositions of mantle-derived melts could be the melting of different mineral phases contained within metasomatic veins trapped within the lithosphere (e.g. Meen *et al.*, 1989; Foley, 1992). The results of melting reactions for the cratonic vein assemblage phlogopite + clinopyroxene + amphibole (Foley *et al.*, 1999) show that amphibole melts completely within 50°C of the solidus and thus the melt compositions are primarily controlled by the composition of the amphibole. Such melts are expected to be richer in SiO_2 and K_2O and poorer in CaO and Al_2O_3 than melts derived from peridotites at similar pressures. Foley *et al.*, however, noted that the consumption of accessory mineral phases such as apatite, ilmenite and rutile can strongly influence melt compositions. The resulting melt from the vein assemblage can infiltrate and react with the surrounding peridotite wall-rock. Mitchell & Edgar (2002) attributed the difference in chemical composition between the phlogopite lamproites from North Table Mountain and madupitic lamproites from Middle Table Mountain to different degrees of partial melting of vein plus wall-rock assemblages.

Geochemical variations in the two types of lamproites from Leucite Hills can also be related to depth of partial melting. The anhydrous kalsilite–forsterite–quartz system has been applied to the origin of lamproites (Kuehner, 1980; Kuehner *et al.*, 1981) to show that madupitic lamproites are generated by lower degrees of partial melting and at greater depths than the phlogopite lamproites. This system, however, has some limitations because it does not contain any Ca-bearing and hydrous phases.

Melting experiments on mantle materials (e.g. Hirose & Kushiro, 1993; Baker & Stolper, 1994; Wasylenki *et al.* 1996; Herzberg *et al.*, 2000) indicate that high-pressure mantle-derived melts normally have higher Fe_2O_3T but lower SiO_2 and Al_2O_3 contents than those generated at lower pressures. An increase in Fe_2O_3T and Tb/Yb and a decrease in Al_2O_3 and SiO_2 of basalts from west to east across the Basin and Range province were thought to indicate shallower melting beneath the western than the central parts (Wang *et al.*, 2002). From the data presented in Fig. 2 it can be seen that the madupitic lamproites have higher Fe_2O_3T and lower SiO_2 and Al_2O_3 contents than the phlogopite lamproites. If these compositional variations can be related to results obtained from the melting experiments of Hirose & Kushiro (1993), Baker & Stolper (1994), Wasylenki *et al.* (1996) and Herzberg *et al.* (2000), then the madupitic lamproite melts were generated at greater depths relative to the phlogopite lamproite.

Variations in melting depths are also supported by the trace element composition, $^{40}Ar/^{39}Ar$ dating, and volumetric proportions of the two lamproite types from the Leucite Hills. Recent high-pressure experimental

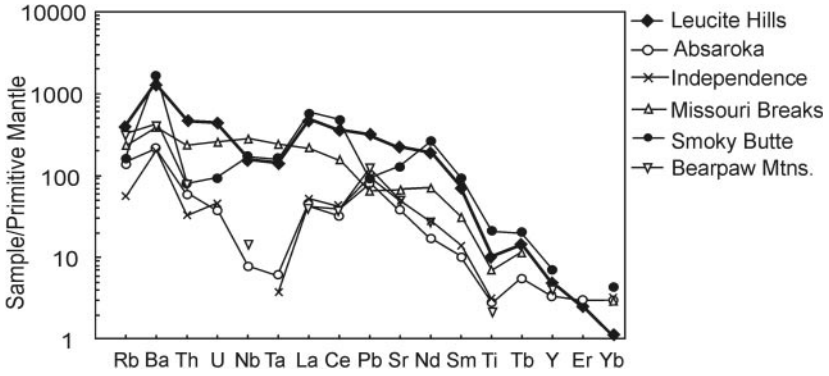

Fig. 8. Trace element patterns of Cenozoic igneous rocks from the Wyoming Province normalized to primitive mantle values (McDonough & Sun, 1995). (Note enrichments in the LILE and negative anomalies in Nb, Ta and Ti, with the exception of the data for the Missouri Breaks rocks.) Data sources: Leucite Hills—this study; Absaroka—Feeley *et al.* (2002); Independence—Meen & Eggler (1987); Missouri Breaks—Scambos (1987); Smoky Butte—Fraser (1987); Bearpaw Mountains—MacDonald *et al.* (1992).

data show that with increasing pressure, clinopyroxene becomes richer in the Ca-Tschermaks component and behaves similarly to garnet in differentiating the REE (Salters & Longhi, 1999). Because melts in equilibrium with garnet have high Tb/Yb values as a result of garnet's stronger preference for HREE and middle REE (MREE) relative to spinel, magmas with high Tb/Yb ratios should be derived from deeper parts of the mantle. From the data presented in Table 3, madupitic lamproites are characterized by marginally higher $(Tb/Yb)_N$ ratios (13·8) than the phlogopite lamproites (10·4). The higher LREE concentration in the madupitic lamproites than in the phlogopite lamproites provides further evidence for a deeper origin for the madupitic lamproites. In addition, the oldest lavas in the Leucite Hills, the madupitic lamproites (3·0–2·5 Ma old) form <1% of the volume of lamproites while the younger phlogopite lamproites (1·8–0·8 Ma old) form >99% (Lange *et al.*, 2000), observations that may indicate that the madupitic lamproites represent the first batch of partial melt generated at greater depths and at lower degrees of partial melting of the mantle source. Although this model might explain the chemical differences between the phlogopite and madupitic lamproites from Leucite Hills, the very different isotopic compositions for the two groups requires that the vein minerals at lithospheric depths must have been out of isotopic equilibrium with the surrounding mantle. Variations in the source mineralogy associated with the depth of partial melting can clearly explain the isotopic compositions of the madupitic and phlogopite lamproites as well as the trends of the isotopic data observed in Figs 9 and 10. Throughout their evolutionary history the two lamproitic melts did not interact with one another, and hence were able to preserve their distinct chemical identities.

LHL IN RELATION TO OTHER CENOZOIC IGNEOUS ROCKS FROM THE WYOMING CRATON

Comparisons between the LHL and other igneous rocks of Eocene to Paleocene age from the Wyoming craton (Fig. 1) are shown in Figs 8–10. These rocks form a number of different magmatic suites, all <55 Ma in age. The Absaroka volcanic province of northwestern Wyoming and southwestern Montana consists of two sub-parallel, NW-trending belts: the western Washburn (andesite, basaltic andesite and dacite) and the eastern Sunlight (shoshonite to latite) volcanic rocks (55–52 and 50–48 Ma, respectively) (Feeley *et al.*, 2002; Feeley & Cosca, 2003). The Independence suite of volcanic rocks, which crops out within the eastern Absaroka volcanic field, is 52–49 Ma old and contains low-K high-alumina tholeiitic basaltic andesite to shoshonite and to high-K dacite (HATS series), and a high-magnesium andesite to banakite (HAB series) (Meen & Eggler, 1987; Harlan *et al.*, 1996). On the northern margin of the Wyoming craton, the Missouri Breaks diatreme (50–45 Ma) contains kimberlite and alnöite (Scambos, 1987), and the Crazy Mountains complex (48 Ma) consists of alkalic malignite, phonolite and trachyte, and subalkalic basalt, andesite and rhyolite (Dudás *et al.*, 1987; Dudás, 1991). The volcanic rocks of the Bearpaw Mountains (54–50 Ma), located in northern Montana, are dominated by minettes and latites (Macdonald *et al.*, 1992), whereas in central Montana, the Highwood Mountains magmatic province (53–50 Ma) consists of quartz-normative latites overlain by flows and intruded by stocks and dikes of potassic mafic rocks (O'Brien *et al.*, 1991). The 27 Ma Smoky Butte lamproite (Marvin *et al.*, 1980), located NE of Leucite Hills, consists of armalcolite–phlogopite and sanidine–phlogopite lamproites (Fraser, 1987; Mitchell

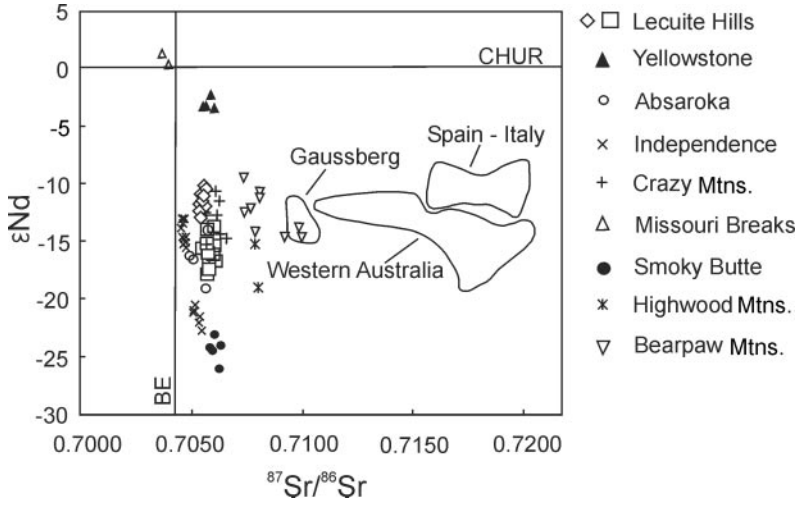

Fig. 9. εNd vs $^{87}Sr/^{86}Sr$ for Cenozoic igneous rocks from the Wyoming craton, and for Gaussberg, Italy, Spain and Western Australia. Data sources: Yellowstone—Hildreth *et al.* (1991); Crazy Mountains—Dudás *et al.* (1987); Highwood—O'Brien *et al.* (1995); other data as in Figs 2, 3 and 9. Open diamonds and squares, madupitic and phlogopite lamproites, respectively.

et al., 1987). About 200 km NW of the Leucite Hills lies the Yellowstone volcanic province, whose activity can be traced over a period of 19 Myr, from southwestern Idaho to the present-day locus of the Yellowstone Plateau (Smith & Braile, 1994). The Yellowstone Plateau and the Snake River Plain volcanic fields, two major products of the Yellowstone hotspot, consist of subalkaline basalt–rhyolite associations (Hildreth *et al.*, 1991).

In a primitive mantle-normalized trace element diagram (Fig. 8) most of the Cenozoic volcanic rocks show Nb, Ta and Ti depletions, except the Missouri Breaks rocks. In terms of their Sr and Nd isotopic compositions, almost all of the Tertiary–Quaternary volcanic rocks from Wyoming plot in the enriched quadrant (excluding the data from Missouri Breaks) and define a near-vertical trend (Fig. 9), with the Yellowstone basalts lying at one end and the Smoky Butte lamproites at the other. Similar to the data from the LHL, those from the Independence volcanic field show large variations in εNd and define two distinct groupings (Fig. 9). It is interesting to note that all of the Cenozoic volcanic rocks from the Wyoming craton have moderately radiogenic Sr isotopic compositions, indicating that the source region of these magmas had time-integrated Rb/Sr slightly higher than that of bulk Earth (BE). It is also clear from Fig. 9 that the isotopic signatures of the alkaline rocks from the Wyoming Province, and hence their sources, are distinct from the K-rich volcanic rocks of Spain, Italy, Gaussberg, and Western Australia.

On a $^{207}Pb/^{204}Pb$ vs $^{206}Pb/^{204}Pb$ diagram the Wyoming Cenozoic igneous rocks plot to the left of the geochron and below the Stacey–Kramers growth line (Fig. 10a). These rocks also plot above the NHRL and form a linear trend on $^{207}Pb/^{204}Pb$ vs $^{206}Pb/^{204}Pb$ and $^{208}Pb/^{204}Pb$ vs $^{206}Pb/^{204}Pb$ diagrams (Fig. 10a and b). The most and least radiogenic Pb isotopic signatures of any of the Tertiary–Quaternary igneous rocks emplaced into the Wyoming craton are from the Missouri Breaks kimberlite–alnöite suite and the Smoky Butte lamproites, respectively. In general, the isotopic variations among the Cenozoic igneous rocks from the Wyoming craton point to a widespread heterogeneous mantle source. No Pb isotope data are available at present for the Absaroka and Bearpaw volcanic rocks.

PETROGENESIS OF THE LHL

Any model proposed for the origin of the LHL has to take into account the following:

(1) higher abundances of MgO, Ni and Cr, and lower abundances of CaO, Al_2O_3 and Na_2O in lamproites relative to most primitive, mantle-derived melts;
(2) the two distinct chemical groupings of the madupitic and phlogopite lamproites;
(3) the LREE enrichment and strongly negative εNd signature of the LHL and some of the other Cenozoic igneous rocks from the Wyoming craton;
(4) the moderately radiogenic Sr isotope compositions of the LHL as well as other Cenozoic igneous rocks from the Wyoming craton despite wide variations in K_2O contents and Rb/Sr ratios;
(5) the Pb isotopic compositions of the LHL and other contemporaneous igneous rocks from the Wyoming craton that plot to the left of the geochron and below the Stacey–Kramers growth line;

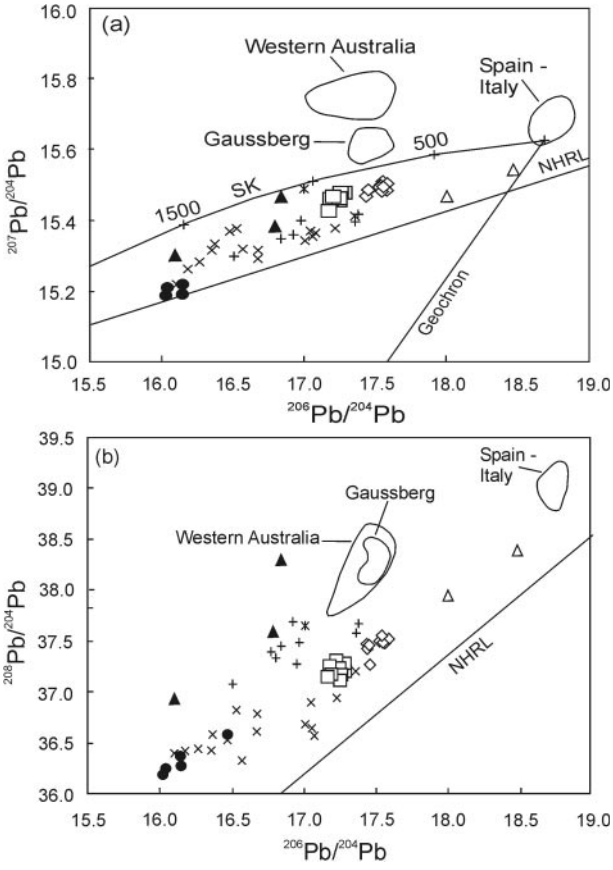

Fig. 10. (a) $^{207}Pb/^{204}Pb$ vs $^{206}Pb/^{204}Pb$, and (b) $^{208}Pb/^{204}Pb$ vs $^{206}Pb/^{204}Pb$ for Cenozoic igneous rocks from the Wyoming craton. Symbols as in Fig. 9. Data sources: Yellowstone—Hildreth *et al.* (1991); Crazy Mountains—Dudás *et al.* (1987); Highwood—O'Brien *et al.* (1995). Other data sources as in Figs 2, 3 and 9. SK, Stacey–Kramers growth line (Stacey & Kramers, 1975). Numbers on the growth line indicate time in Ma. NHRL, Northern Hemisphere Reference Line (Hart, 1984).

(6) the presence of both small- and large-scale source heterogeneity, reflected by the variations in the Sr–Nd–Pb isotopic compositions of the LHL and other Cenozoic volcanic rocks found throughout the Wyoming craton;
(7) the Nb, Ta and Ti depletions and LILE enrichments of the LHL as well as other Cenozoic volcanic rocks from the Wyoming craton.

On the basis of these observations, we propose a three-stage model (Fig. 11) involving: (1) major melt removal from the Wyoming upper mantle in the Archean (~2·8 Ga) that left behind a refractory and depleted sub-continental mantle lithosphere; (2) ancient (>1 Ga) metasomatism of the sub-continental mantle related to subduction of crustal materials; (3) recent (<100 Ma) metasomatism of the sub-continental lithosphere during mantle upwelling leading to K enrichment and subsequent melting of the metasomatized portions of the mantle source.

Depletion processes

The low abundances of Al_2O_3, SiO_2, and CaO and the high MgO, Ni and Cr contents of the studied samples (Tables 2 and 3) are consistent with the geochemical characteristics of other lamproites (e.g. Bergman, 1987; Foley, 1992), supporting derivation of the LHL from a major-element depleted mantle source, dominantly harzburgitic in composition. In addition, the relatively low HFSE and HREE contents of the LHL are common among lamproites and a variety of other alkaline igneous rocks from Wyoming and are generally thought to indicate mantle source depletion by previous partial melting events (Eggler *et al.*, 1988; O'Brien *et al.*, 1995). Although the low concentrations (see Table 3) of Tm (<0·2 ppm), Yb (<0·9 ppm) and Lu (<0·11 ppm) in the LHL probably indicate residual garnet in the source, calculations by Tainton & McKenzie (1994) show that to account for these concentrations, the mantle source of the lamproites must have been depleted by extensive melting.

The involvement of a refractory (harzburgitic) mantle source for lamproites is supported by data from mantle xenoliths and phase equilibria studies. Although mantle xenoliths are exceptionally rare in lamproites, those so far recovered are dominantly dunite and garnet harzburgite (Atkinson *et al.*, 1984; Eggler *et al.*, 1987; Mitchell & Bergman, 1991; Carlson & Irving, 1994). Refractory mantle xenoliths, dominantly harzburgites, have been reported from the Colorado–Wyoming kimberlites (Eggler *et al.*, 1987), and from the Williams kimberlite, associated with a more extensive Eocene suite of alkalic ultramafic intrusions in the Missouri Breaks; these indicate that much of the lithospheric mantle is depleted in magmatophile elements (i.e. Ca, Al and Fe) (Carlson *et al.*, 1999). In addition, ultramafic xenoliths from the Bearpaw Mountains are composed mainly of harzburgites, and rare dunites and werhlites, with major element compositions moderately to extremely depleted relative to the chemical composition of average peridotite from the sub-continental lithosphere (Downes *et al.*, 2004). Most of the published phase equilibrium data for natural lamproites (e.g. Foley, 1993; Mitchell, 1995*a*; Edgar & Mitchell, 1997; Mitchell & Edgar, 2002), as well as studies of anhydrous and volatile-bearing (H_2O, CO_2, F) compositions in the synthetic system kalsilite–forsterite–quartz at high pressures also point to harzburgitic protoliths as the mantle source of ultrapotassic melts (Kuehner, 1980; Foley *et al.*, 1986).

Generation of a refractory harzburgitic mantle beneath the Wyoming craton can be attributed to the formation of continental crust at between 3·5 and

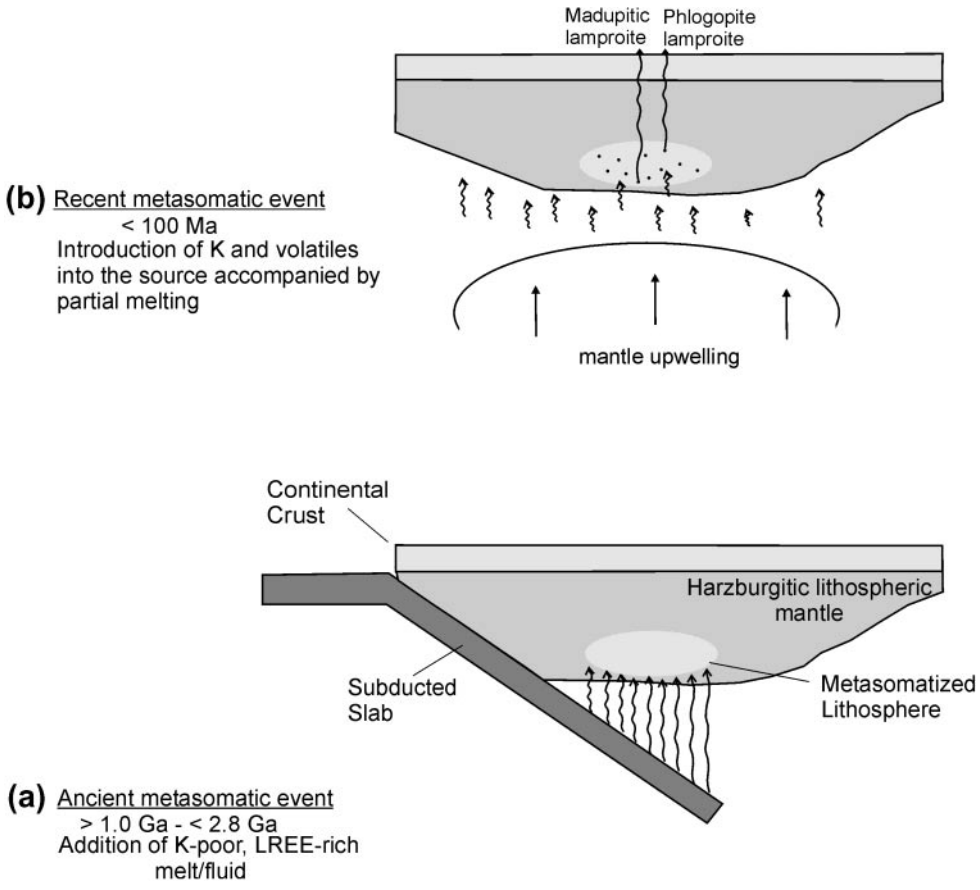

Fig. 11. Summary of the metasomatic stages that contributed to the source evolution of the LHL. (a) Ancient metasomatic event; (b) recent metasomatic event.

2·5 Ga, as indicated by the ages of the Granite Mountain gneisses (Wooden & Mueller, 1988) and the Wind River Range granites (Stuckless *et al.*, 1985; Frost *et al.*, 1998). Based on geothermobarometry calculations on mantle xenoliths from Wyoming–Colorado kimberlites, Eggler *et al.* (1987) proposed that the entire Wyoming subcontinental mantle to the depth of at least 200 km was depleted during a melting event or events in the Precambrian. Those workers argued that although the Front Range granitic batholiths have been dated at 1·4 and 1·0 Ga (Peterman *et al.*, 1968), they largely reflect remobilization of pre-existing crust. This, coupled with the lack of widespread basaltic volcanism during the Proterozoic, might suggest that the depletion event was restricted to the Archean. Additional evidence for Archean crustal extraction comes from mafic crustal xenoliths from the Leucite Hills. Based on geochemical compositions and whole-rock Pb–Pb and Sm–Nd pseudoisochrons (Mirnejad & Bell, in preparation) and U–Pb dating of zircons (Farmer *et al.*, 2005) indicating ages of about 2·8 Ga, these rocks are interpreted to represent fragments of igneous material intruded into the deep crust and thus support the Archean depletion of the Wyoming upper mantle. Other support for Archean depletion is given by Os isotopic ratios of spinel peridotite, pyroxenite and glimmerite xenoliths in Eocene minette dikes from southern Montana that yield model ages of 2·7 to 2·9 Ga (Carlson & Irving, 1994; Rudnick *et al.*, 1999). Although mantle xenoliths from the Bearpaw Mountains have provided somewhat younger (2·45–1·13 Ga) Nd model ages (Carlson & Irving, 1994; Downes *et al.*, 2004), these might represent a mixed age intermediate between that of the Archean depletion event and a younger LREE enrichment event.

Enrichment processes

The mantle source of the LHL clearly experienced enrichment as witnessed by the high alkali metal and LREE contents (Table 3), extremely negative εNd values, and high Ba/Nb, Ba/La, Nb/Pb and Ce/Pb ratios.

Lamproites, along with kimberlites, are the most extreme products of mantle enrichment processes

(Hawkesworth *et al.*, 1985) and of the many hypotheses proposed to produce the high incompatible element and volatile contents in their mantle source, metasomatism is the most widely accepted (e.g. Menzies & Wass, 1983; Hawkesworth *et al.*, 1985; Foley *et al.*, 1986; Menzies, 1987; Menzies & Hawkesworth, 1987). The addition of hydrous melts or fluids enriched in K_2O and incompatible elements to the mantle source is a prerequisite for the generation of lamproitic melts (Hawkesworth *et al.*, 1990). Based on melting experiments of primary lamproites and the near-solidus phase relationships at high *P–T* conditions (4–7 GPa, 1000–1200°C; Foley, 1992), phlogopite ± richterite ± clinopyroxene ± apatite ± titanate are considered to be the main minerals making up the metasomatic veins in the lamproite mantle source (Foley, 1993; Mitchell, 1995*a*; Edgar & Mitchell, 1997; Mitchell & Edgar, 2002). In addition, the stability of hydrous phases under upper mantle conditions has been experimentally investigated by a number of workers (e.g. Kushiro *et al.*, 1967; Tronnes *et al.*, 1988; Konzett *et al.*, 1997; Sato *et al.*, 1997), demonstrating that phlogopite and amphibole can be stable throughout the cratonic lithosphere. Carlson & Irving (1994) and Rudnick *et al.* (1999) reported glimmerite veins composed of mica, apatite, orthopyroxene, clinopyroxene, rutile, zircon, monazite, magnetite, and chromite that cut harzburgitic xenoliths contained in potassic volcanic rocks in the Highwood Mountains. In addition, Carlson & Irving (1994) have indicated that most peridotite xenoliths from the Highwood Mountains contain mica and amphibole. It is generally agreed that vein assemblages formed during metasomatism of the mantle contribute greatly to the major and trace element budgets of potassic or ultrapotassic melts (Luth *et al.*, 1993; Schmidt *et al.*, 1999).

Enrichment processes leading to the formation of metasomatic mantle minerals are diverse and can be caused by the reaction of mantle rocks with metasomatic fluids or melts derived from the dehydration or partial melting of subducted slabs (Hawkesworth *et al.*, 1990; Murphy *et al.*, 2002), or volatiles or melts that emanate from mantle upwellings (McKenzie, 1989; Tainton & McKenzie, 1994). On the basis of our findings we propose that both an early metasomatism of the lithospheric mantle source related to subduction processes and a contribution from a recent mantle upwelling or plume were involved in the enrichment of the mantle below the Wyoming craton.

Ancient metasomatic event

An ancient metasomatic event in the mantle source is indicated by the extremely negative εNd values of the LHL (Fig. 9). With regard to the approximate timing of this enrichment event, both late Archean and mid-Proterozoic have been cited as the age of metasomatism. Vollmer *et al.* (1984) argued that metasomatism took place during stabilization of the Archean lithosphere in the Wyoming Province at about 2·7 Ga and showed that slight enrichment in Nd/Sm and Rb/Sr ratios in the upper mantle was sufficient to generate the observed Nd and Sr isotopic variations seen in the LHL. Even the Pb isotopic data for the Leucite Hills and Smoky Butte lamproites are consistent with ancient metasomatism; these data plot to the left of geochron and below the Stacey–Kramers growth line (Fig. 10a) indicating U/Pb and Th/Pb fractionation of their sources. Based on the isotopic compositions of the Smoky Butte lamproites, Fraser (1987) and Mitchell *et al.* (1987) suggested that depletion of U, Th and Pb in the source occurred subsequent to a 2·5 Ga metasomatic event that enriched the Wyoming mantle in LREE, U, Th and Rb. Archean enrichment of the Wyoming lithosphere has also been documented from potassic mafic magmas of the Highwood Mountains (O'Brien *et al.*, 1995), involving an increase in Ba/Nb and Ba/La, and decrease in Nb/Pb and Ce/Pb ratios along with a decrease in εNd values from –11 to –20. Not all of the evidence, however, supports Archean enrichment. The Os, Sr, Nd and Pb isotopic compositions of mica harzburgite xenoliths, and zircon and monazite dates from glimmerite veins from the Highwood Mountains give ages of about 1·8 Ga, indicating a mid-Proterozoic enrichment event (Carlson & Irving, 1994; Rudnick *et al.*, 1999). Some additional Rb–Sr model ages for phlogopite from the Bearpaw Mountains mantle xenoliths yield values of about 1·25 Ga (Downes *et al.*, 2004), and model ages for mafic alkalic and subalkalic rocks from the Crazy Mountains fall between 1·3 and 1·8 Ga (Dudás *et al.*, 1987; Dudás, 1991). Metasomatic Nd model ages of ~2·2–2·0 Ga (Feeley, 2003) were obtained from mafic lavas from Sunlight and Washburn volcanoes. Eggler *et al.* (1988), on the basis of model Nd ages (T_{DM}) of a variety of Tertiary igneous rocks from the Wyoming craton, came to a similar conclusion. Websterite and pyroxenite mantle xenoliths from the Wyoming–Colorado kimberlite pipes were interpreted by Eggler *et al.* (1987) as representing metasomatic zones created during an enrichment event, during either the Archean or the Proterozoic (1·6–1·7 Ga). The εNd values for the madupitic and phlogopite lamproites from the Leucite Hills are much too low to have been generated from a non-metasomatized, harzburgitic source, suggesting that the Sm/Nd ratio must have been lowered by metasomatism. Model ages calculated for the LHL samples from this study, assuming a CHUR reservoir, correspond to 715 Ma for the madupitic lamproites and 1034 Ma for the phlogopite lamproites. These 'ages' represent minimum limiting values, and give support to an old metasomatism of the mantle source associated with LREE enrichment. Given the

different estimates of the timing of enrichment of the Wyoming lithosphere, and the possibility of more than one period of metasomatism, we refer to this >1 Ga episode as the ancient metasomatic event.

The similar trace element patterns of the LHL and other Tertiary volcanic rocks emplaced within the Wyoming craton (excluding Missouri Breaks) (Fig. 8) suggest that the enrichment of their mantle sources may be related. The Nb, Ta and Ti depletions and the LILE and LREE enrichment of the LHL closely resemble those observed in convergent margin tectonic settings (Pearce, 1982; Cox, 1988; Hawkesworth *et al.*, 1990), indicating that the metasomatic signature in their mantle source was probably subduction-related. In addition, the average Ce/Pb ratio (17) of the LHL is much lower than that of mid-ocean ridge basalts (MORB) and ocean island basalts (OIB) (25), supporting the involvement of fluids or melts from subducted crustal materials.

Although lamproites are rarely found in convergent tectonic settings and few can be linked to modern subduction zones, the patterns of source enrichment indicated by the trace element and Sr–Nd–Pb isotopic compositions of the LHL nevertheless would suggest subduction-related processes (Fig. 8). In this context, Bergman (1987) noted that lamproites are commonly located above fossil Benioff Zones and Mitchell & Bergman (1991) suggested that the tectonic settings and compositional characteristics of lamproites such as Nb and Ta depletion and LILE and LREE enrichment point to the involvement of ancient subducted slabs. Other evidence from Tertiary igneous rocks in the Wyoming Province supports subduction-related mantle metasomatism, including xenocrystic plagioclase and granitic melt inclusions in zircons from glimmerite veins that cut harzburgite xenoliths, as well as crust-like REE patterns, and Nb depletions of xenoliths from the Highwood Mountains (Rudnick *et al.*, 1999). Both Carlson & Irving (1994) and Rudnick *et al.* (1999) used zircon and monazite ages of about 1·8 Ga from these glimmerite veins to date the involvement of an old subduction process. An increase in Ba/Nb, Ba/La, Nb/Pb and Ce/Pb ratios and a decrease in εNd values among the Highwood volcanic rocks were considered by O'Brien *et al.* (1995) as evidence that the ancient metasomatic signatures in their mantle source are subduction-related.

It is clear from the Sr–Nd isotopic diagram (Fig. 9) that the LHL plot in the enriched quadrant, and in the case of Pb (Fig. 10) to the left of the geochron and below the Stacey–Kramers growth line. The observed Pb isotopic variation can be attributed to the extent to which U/Pb ratios are fractionated during subduction. It is possible that high O_2 fugacity during subduction oxidized U^{4+} to the more soluble U^{6+} and caused U to be lost relative to Pb, thus lowering the U/Pb ratio in a downgoing slab (White & Dupré, 1986). The Pb, Sr and Nd isotopic signatures of the LHL can also be attributed to the chemical heterogeneity of subducted materials, such as crustally derived sediments containing carbonate and phosphate. Because of their low Rb/Sr, U/Pb ratios, and relatively high Nd/Sm ratios (e.g. Othman *et al.*, 1989; Plank & Langmuir, 1998) any fluids or melts derived from such sediments can metasomatize the lithosphere and generate the low time-integrated Nd, Sr and Pb isotopic ratios found in the Leucite Hills lamproites.

There is also field evidence for late Archean or mid-Proterozoic subduction beneath the Wyoming and adjacent cratons. Based on geochemical data and geological observations, Mueller & Wooden (1988), Wooden & Mueller (1988), Frost *et al.* (1998) and Chamberlain *et al.* (2003) have suggested that the Wyoming craton may have been the site of a long-lived, late Archean, convergent continental margin. Evidence for Archean subduction includes compositionally diverse, late Archean andesitic amphibolites in the Beartooth Mountains in Wyoming (Mueller *et al.*, 1983) with trace element patterns that closely resemble those of modern arc magmas. A number of late Archean supracrustal sequences (mafic volcanic rocks, metagraywackes, pelitic schists, and minor intermediate to felsic volcanic rocks and quartzites) preserved within the southern and western portions of the Wyoming Province are consistent with intracratonic and cratonic margin settings for basin development that occurred during crustal growth along the SW margin of the Wyoming Province (Chamberlain *et al.*, 2003). As an alternative, Bennet & De Paolo (1987), Hoffman (1989), and Bickford *et al.* (1990), have suggested that the western United States experienced collisional tectonics and associated magmatism during the mid-Proterozoic (1·85–1·65 Ga). U–Pb zircon geochronology of metasomatized mantle xenoliths from the Great Falls tectonic zone in the NW margin of the Wyoming craton led Carlson & Irving (1994), Carlson *et al.* (1999) and Rudnick *et al.* (1999) to propose a model in which metasomatism of the Archean lithospheric mantle of the Wyoming craton was associated with the creation of the Great Falls tectonic zone, accompanied by accretion of mobile belts to its northern boundary around 1·8 Ga.

In summary, subduction of crustal materials (including sediments) during either the late Archean or mid-Proterozoic seems to be the most likely process responsible for the metasomatism of the lithospheric keel beneath the Archean Wyoming craton prior to 1·0 Ga.

Recent metasomatic event

In addition to Archean depletion and ancient (>1 Ga) enrichment events, there is also sufficient evidence for

the involvement of recent (<100 Ma) metasomatic activity affecting the Wyoming mantle.

Most lamproites worldwide have radiogenic Sr isotopic compositions indicating high, long time-integrated Rb/Sr ratios in their source (Fig. 4). McCulloch *et al.* (1983) ascribed the highly radiogenic Sr isotopic compositions of lamproites from Western Australia to Proterozoic (>1 Ga) Rb enrichment relative to Sr. The $^{40}Ca/^{42}Ca$ ratios of the Sisimiut lamproites, West Greenland (Nelson & McCulloch, 1989), indicate that K_2O enrichment within their mantle source occurred at least 1 Gyr prior to lamproite eruption. In contrast, however, the $^{87}Sr/^{86}Sr$ ratios of the LHL are only moderately radiogenic and this may indicate that the ancient metasomatism produced a mantle source characterized by low Rb/Sr ratios. Carlson & Irving (1994) considered mantle xenoliths with high negative εNd values and moderately radiogenic Sr isotopic ratios from the Highwood Mountains as evidence for ancient metasomatism characterized by low Rb/Sr and Nd/Sm ratios. Such geochemical characteristics, common among all the Cenozoic igneous rocks from the Wyoming craton (Fig. 10), including those of Smoky Butte and the Absaroka volcanic province, have been attributed by Mitchell *et al.* (1987) and Feeley (2003) to insignificant amounts of Rb being added to the mantle source during the ancient metasomatic event.

The relatively low $^{87}Sr/^{86}Sr$ ratios and thus low time-integrated Rb/Sr ratios in the source of the LHL are seemingly at odds with the relatively high K_2O and Rb contents of the lamproites. Examples of enrichment in K_2O without accompanying Sr isotopic enrichment are also indicated by the highly K_2O-enriched lavas from the Sunda arc of Indonesia (Wheller *et al.*, 1987). The marked differences between the $^{87}Sr/^{86}Sr$ ratios in the West Kimberley and Smoky Butte lamproites (see Fig. 9) was considered by Mitchell *et al.* (1987) to reflect different styles of metasomatism, with the Smoky Butte source containing more richterite and titanite and less phlogopite than the West Kimberley source. Mitchell *et al.* (1987) also emphasized that alumina-deficient and K_2O-poor richterites are unable to provide sufficient Al_2O_3 and K_2O to account for the abundant phlogopite and sanidine contained in the Smoky Butte lamproites, and suggested recent introduction of phlogopite into the mantle source of the Smoky Butte lamproites during volatile fluxing in the Tertiary as a more viable explanation for the different styles of enrichment between the Smoky Butte and West Kimberley lamproites. A similar argument can thus be used to explain the differences in Sr isotope compositions between the Leucite Hills and West Kimberley lamproites.

The whole-rock oxygen isotope data show that the $\delta^{18}O$ values of the LHL ($\delta^{18}O = +8$ to $+9‰$ Table 4) are higher than mantle values ($\delta^{18}O = +5{\cdot}5‰$ Mattey *et al.*, 1994). Our $\delta^{18}O$ data are very similar to the values of $+8{\cdot}8‰$ reported by Kuehner (1980) for phlogopite phenocrysts from the LHL. Because high-level, crustal contamination is ruled out in the petrogenesis of the LHL, the $\delta^{18}O$ of the phlogopite phenocrysts may be considered a source feature and probably reflects recent metasomatic activity associated with hydrous fluids or melts. Further evidence for the recent addition of K_2O to the source of the LHL may come from the lack of correlation between the K_2O contents and Nd isotopic ratios of the studied samples. As with the LHL, the Washburn and Sunlight mafic rocks from the Absaroka volcanic province show wide variations in K_2O, LILE, LREE contents and Rb/Sr ratios with no correlation with $^{143}Nd/^{144}Nd$ ratios, features that are consistent with recent (<100 Ma) mantle metasomatism (Feeley, 2003). As can be seen in Fig. 12, there is no correlation between εNd values and K_2O contents of the Cenozoic igneous rocks from the Wyoming craton. This is strong evidence that the K_2O enrichment of the Wyoming mantle source was independent of the ancient LREE enrichment, and that the addition of K_2O probably occurred during a much younger metasomatic event. The question as to why Sr–Nd–Pb isotopes were not affected by the recent metasomatic activity remains to be answered, but it could be that the K-bearing fluid phase had very low Nd, Sr and Pb contents.

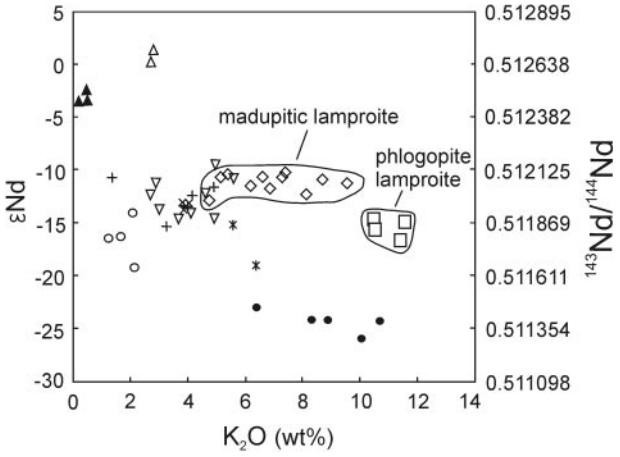

Fig. 12. Variation of εNd vs K_2O (wt %) for the Cenozoic igneous rocks from the Wyoming craton. [Note the absence of any correlation between εNd and K_2O (wt %).] Symbols and data sources as in Fig. 9.

Other evidence for recent metasomatism in the region includes the presence of undeformed phlogopite in mantle xenoliths from the Bearpaw Mountains (Downes *et al.*, 2004) that was introduced after tectonism and before incorporation of the xenoliths into their host magmas, perhaps during the early Tertiary. Also, Carlson *et al.* (1999) have noted that the Sr, Nd and Pb isotopic compositions of clinopyroxenes in some of

the peridotite xenoliths from the Williams kimberlite overlap those of alkalic magmas from the Montana high-K igneous province, and concluded that these pyroxenes were introduced by metasomatism shortly before the capture and transport of the xenoliths. Those workers also attributed small veins of phlogopite in some xenoliths to recent metasomatic activity.

Although there is abundant evidence to support the existence of recent metasomatic activity that led to the addition of K and volatiles to the mantle source of the LHL, the ultimate source of the potassium, and the reasons for preservation of the older isotopic signatures need to be answered. These issues are discussed in the following sections.

Lithospheric vs sub-lithospheric sources

Isotopic and trace element variations among the Cenozoic igneous rocks from the Wyoming craton (excluding the Missouri Breaks) fall outside the known ranges of OIB and therefore their parental melts cannot be derived solely from a normal, sub-lithospheric mantle source. Moreover, for metasomatic minerals to retain their geochemical integrity from the time of the ancient metasomatic event they need to be preserved in a reservoir that has been isolated from the convecting mantle for a long period of time. Such a reservoir could be located in the rigid sub-continental lithosphere, within the mantle Transition Zone or even the lower mantle.

In those models for lamproite petrogenesis involving the Transition Zone, subducted continentally derived sediment, stored for long periods of time at the base of the upper mantle (~650 km), can undergo partial melting and provide melts capable of metasomatizing the mantle. Ringwood *et al.*'s (1992) model for the origin of kimberlites and lamproites involved subducted sediments that formed a garnetite layer within the Transition Zone. Generation of partial melts within the Transition Zone as a result of convection currents from the lower mantle resulted in an LREE-enriched melt capable of metasomatizing the overlying depleted mantle. Ringwood *et al.* (1992), based on experiments using a synthetic Group I kimberlite, showed that at 16 GPa and 1650°C, corresponding to *P–T* conditions within the Transitions Zone, majorite garnet (13% Al_2O_3) and β-M_2SiO_4 were the liquidus or near-liquidus phases. Majorite garnet inclusions in diamond (Moore & Gurney, 1991) and exsolution features in garnet–clinopyroxene xenoliths from the Jagersfontein kimberlites (Haggerty & Sautter, 1990) provided additional evidence that the garnet originally contained a majorite component. Ringwood *et al.* (1992) argued that the Transition-Zone model could apply to lamproite petrogenesis because of the geochemical similarity between olivine lamproites and Group II kimberlites.

Although there is now abundant seismic tomographic evidence for the accumulation of subducted oceanic slabs at the 650 km discontinuity (e.g. Simons *et al.*, 1999; Fukao *et al.*, 2001), the assumption that lamproites can originate from such sources should be treated with caution. The Jagersfontein kimberlites from which majorite garnets were recovered are Group I kimberlites; these do not share the distinctive geochemical characteristics of lamproites and Group II kimberlites (Smith, 1983; Mitchell, 1989, 1995*b*; Skinner, 1989). Moreover, olivine is dominantly a xenocryst phase in olivine lamproites and thus the compositions of olivine lamproites do not reflect those of their parental magmas (Mitchell, 1995*a*). In addition, Tainton & McKenzie (1994) argued that because the majorite garnet exsolution rate constants are unknown, estimates of the time taken for majorite exsolution from garnet cannot be made. Therefore, the majorite garnet inclusions are, at present, only evidence that diamonds, rather than kimberlites, form in the Transition Zone (Tainton & McKenzie, 1994). Although Ringwood *et al.* (1992) reported high-pressure, near-liquidus garnet and clinopyroxene phases, the chemical compositions of these minerals differ from those of the eclogites or garnetite found as xenoliths in kimberlites (Edgar & Mitchell, 1997). Many high *P–T* melting experiments on lamproites do not confirm a garnetite source but point to the presence of phlogopite, K-rich amphibole and apatite (Foley, 1992; Mitchell, 1995*a*; Edgar & Mitchell, 1997; Mitchell & Edgar, 2002) that are necessary to account for the extreme chemical compositions of lamproites and their volatile contents. Experiments on the stability of phlogopite and K-amphibole under upper mantle conditions (e.g. Kushiro *et al.*, 1967; Konzett *et al.*, 1997; Sato *et al.*, 1997) show that phlogopite and amphibole can be stable in the sub-cratonic mantle only to depths of about 250 km.

The model proposed by Murphy *et al.* (2002) to explain the petrogenesis of the Gaussberg lamproites in the East Antarctic shield is similar, in many ways, to that of Ringwood *et al.* (1992), involving the melting of subducted, Archean continent-derived sediments stored within the Transition Zone or lower mantle for 2–3 Gyr. In this model, the main potassium-bearing phase at such depths is K-hollandite. Murphy *et al.* (2002) argued that the low εNd values of the Gaussberg lamproites require long-term source enrichment in the LREE, and the Pb isotope compositions that plot to the left of the geochron indicate U/Pb fractionation during Archean subduction of sediments into the Transition Zone. One of the more important objections made by Murphy *et al.* (2002) to metasomatism of the Gaussberg sub-continental lithosphere is the lack of any geochemical evidence for recent

enrichment. This is not true for the LHL because of the evidence for the recent metasomatism in their mantle source.

The lack of widespread ultrapotassic magmatism in oceanic environments and the confinement of kimberlites and lamproites to mantle sources associated with Archean cratons (White *et al.*, 1995; Jaques & Milligan, 2004) indicate that the origin of lamproites and kimberlites is controlled by thickened lithosphere. Phase equilibria studies suggest that lamproites originate from partial melting of veined mantle sources at 4–7 GPa and 1000–1200°C (Foley, 1993; Mitchell, 1995*a*; Edgar & Mitchell, 1997; Mitchell & Edgar, 2002), *P–T* conditions that are very different from those in the Transition Zone. Moreover, the fact that the isotopic compositions of some xenoliths from the sub-continental mantle lithosphere overlap with those of lamproites might be consistent with sub-continental mantle lithosphere as the ultimate source of lamproites (Wilson, 1989).

Geodynamic setting

Recent metasomatism and subsequent partial melting of the Wyoming mantle can be explained by (1) shallow subduction of the Farallon plate under the Wyoming sub-continental lithosphere, or (2) upwelling of mantle materials during lithospheric extension. These are discussed in turn.

The traditional interpretation of Cenozoic magmatism in the western USA is that active subduction of the Farallon plate led to the generation of a series of mantle-derived magmas (e.g. Lipman, 1980; Bird, 1984). However, more recent models involve mixing between partial melts of ancient metasomatized lithosphere and asthenospheric melts that migrated upward as the result of slab roll-back or slab break-off associated with flat subduction of the Farallon plate (Madsen *et al.*, 2006). For example, the arc-like geochemical characteristics of the Tertiary–Quaternary volcanic rocks of the Wyoming craton, including those from the Elkhead Mountains (Leat *et al.*, 1988), the Highwood Mountains (O'Brien *et al.*, 1991, 1995) and the Absaroka volcanic fields (Feeley, 2003; Feeley & Cosca, 2003) are attributed to metasomatism of the overlying asthenosphere during flat subduction of the Farallon plate in the late Cretaceous.

The existence of the Farallon plate beneath the Montana–Wyoming area and thus enrichment of the mantle wedge during Farallon plate subduction is questionable. To relate the Tertiary–Quaternary magmatism in the Wyoming craton to Farallon plate subduction, the subduction zone must have extended at least 1200 km inland from the continental margin and the angle of subduction would have to have been unusually shallow (e.g. Severinghaus & Atwater, 1990; Lee, 2005). Although Murphy *et al.* (2003) and Ihinger *et al.* (2004) considered that overriding of a mantle plume by the Pacific oceanic plate at ~50 Ma resulted in shallowing of the subduction zone, the problem with such a model is the distance between the easternmost limit of Eocene magmatism and the inferred location of the trench (~1500 km to the west), which exceeds the maximum width of the Andean cordillera associated with flat slab subduction. In addition, the thick and coherent lithospheric mantle beneath the Wyoming craton would have stood as a physical impediment to flat-slab subduction (Dudás, 1991). Heat-flow patterns (Blackwell, 1991), geothermobarometric calculations from xenoliths (Eggler *et al.*, 1987), and seismic tomography data (Artemieva & Mooney, 2001, and references therein) support the presence of thick continental lithosphere beneath the Wyoming craton. Even if the Farallon slab was able to subduct underneath the Wyoming craton, it would have remained in contact with colder lithosphere, probably precluding partial melting. It is more likely that the dominant arc-like geochemical characteristics of the Tertiary volcanic rocks from Wyoming, including those of the LHL, are inherited from an ancient metasomatic component (>1 Ga) in the lithospheric mantle. Fitton *et al.* (1988) and Hergt *et al.* (1991) have demonstrated that Nb, Ta and Ti depletions as well as high LILE/HFSE and LREE/HFSE ratios in continental igneous rocks not associated with contemporary subduction systems may preserve a record of the effects of older subduction in the sub-continental lithosphere.

An alternative to models that attribute recent metasomatism to flat subduction of the Farallon plate is recent metasomatism and partial melting of the sub-continental lithosphere by a mantle upwelling or a plume. The Yellowstone hotspot is the only possible candidate for mantle plume activity in Wyoming (e.g. Smith & Braille, 1994; Camp, 1995; Schutt *et al.*, 1998; Smith & Siegel, 2000). Mitchell & Bergman (1991) have stressed the close relationship between the Leucite Hills magmatism and Yellowstone hotspot activity, and suggested that the onset of partial melting in the mantle source of the LHL coincided with the time when the outer parts of the Yellowstone hotspot track passed by the Rock Springs region at 1–2 Ma. Edgar (1983) investigated the relationship between the K/(K + Na) (molecular ratio) and the Ba content of ultrapotassic rocks from the western USA with distance from the Yellowstone hotspot and noticed that the LHL situated closest to Yellowstone have the highest K/(K + Na) and Ba contents. In the model of Edgar (1983), K was introduced from the Yellowstone plume and transported by fluids into the upper mantle.

A difficulty with the hotspot or plume model is the lack of temporal and spatial evidence for the presence of the

Yellowstone plume beneath the various volcanic centres in Wyoming. If the Yellowstone plume induced partial melting in the mantle source that generated all of the Tertiary–Quaternary magmatism in Wyoming, then the plume must have existed beneath the Wyoming lithosphere for the last 55 Myr. However, the oldest age proposed for the Yellowstone plume is 19 Ma, an age that marks the time when it emerged near the Oregon–Nevada border (Smith & Braile, 1994; Zoback *et al.*, 1994), much further NW of the present Yellowstone hotspot. Plate reconstructions by Murphy *et al.* (2003) suggest that at 50 Ma the Yellowstone plume was probably beneath the Pacific ocean floor, close to the continental margin of western North America. It seems unlikely, but not impossible, that at 50 Ma such a plume, located thousands of kilometers to the west of the Bearpaw, Highwood and Smoky Butte localities, could have played a role in the enrichment and partial melting of the mantle source underlying these volcanic fields. Another major drawback to the involvement of a mantle plume are the recent arguments that question the fueling of the Yellowstone hotspot by a plume of hot material rising from the lower mantle (Walker *et al.*, 2004; Anderson, 2005). According to Christiansen (1993), the relations between rift zones in the surrounding areas and the propagation of the Yellowstone hotspot from 19 Ma to the present time appear to be inconsistent with the geometry of a deep mantle plume. In addition, seismic tomography data have not revealed vertical structures with low velocity extending into the lower mantle but a low-velocity body beneath Yellowstone that appears to be restricted to the upper mantle (Christiansen *et al.*, 2002). Anderson (2005), using the polling approach of Courtillot *et al.* (2003), also concluded that the plume hypothesis for the Yellowstone hotspot scores poorly against an asthenospheric feature associated with stress release induced magmatism.

As an alternative model, the thermal anomaly beneath the thick Wyoming lithosphere could have been created by mantle upwelling independent of plume activity. As favoured by Dudás (1991) for the Crazy Mountains volcanic rocks, the upwelling of mantle below the Wyoming craton could be the result of back-arc extension and lithospheric thinning (decompression) related to Farallon plate subduction (Eggler *et al.*, 1988; Christiansen *et al.*, 2002). Contemporaneous with lithospheric extension, episodic mantle upwelling resulted in partial melting of the heterogeneous Wyoming sub-continental lithosphere that generated most of the Cenozoic magmatism. Beneath Archean cratons, convective upwelling in the underlying sub-lithospheric mantle has been inferred to occur on average every few million years (Foley *et al.*, 1999); thus several partial melting events could have occurred in the mantle. The lithospheric mantle is too cold to melt and perturbation of the mantle solidus by a heat source and/or volatile influx is required before partial melting takes place. A mantle upwelling can spread beneath the lithosphere and raise the temperature to 100–200°C above normal by conduction (White & McKenzie, 1989). However, this is a slow process and more efficient transport of heat as well as volatiles or melts occurs when the upwelling mantle moves upwards through lithospheric channels and fractures (Ebinger & Sleep, 1998), in which case the upwelling mantle viscosity needs to be relatively low (Albers & Christensen, 2001; Xue & Allen, 2005).

Many of the problems associated with the origin of the LHL and their mantle source are analogous to those associated with the petrogenesis of ultrapotassic rocks in Italy; both rock types show depletions in Nb, Ta and Ti, enrichment in the LREE, high Mg-numbers and decoupling between isotopic compositions and some major and trace element abundances. A common feature of both groups of rocks is the involvement of at least two isotopically distinct sources. Continuing debate centres around whether Cenozoic magmatism in Italy is related to subduction or to large-scale plume activity [see discussions by Peccerillo & Lustrino (2005) and Bell *et al.* (2006) and references therein], similar to the types of models proposed for the origin of the LHL.

The distinct differences in the chemical compositions of the madupitic lamproites and the phlogopite lamproites from the Leucite Hills probably result from variations in the source mineralogy and the depth of partial melting in the metasomatized lithosphere. As discussed previously, the relative volumes of the two groups of lamproites and their temporal and geochemical relationships indicate that the madupitic lamproite magma was generated prior to and at greater depths than the phlogopitic lamproite melts. The heat and volatiles recently introduced by transported materials from the upwelling mantle initially induced metasomatism and partial melting (madupitic lamproites) in the deeper parts of the sub-continental lithosphere. By propagating to shallower levels, the upwelling material underwent further partial melting that resulted in the phlogopite lamproite magmas.

CONCLUSIONS

The two major types of lamproite in the Leucite Hills, madupitic and phlogopite lamproites, show distinct characteristics in many major and trace element and Sr–Nd–Pb isotope diagrams. Although fractional crystallization or crustal contamination has had a minimal effect, variations in the source mineralogy and the depth of partial melting appear to have played an important role in the petrogenesis of the lamproites.

The mantle source involved in generating the LHL has clearly undergone both depletion and enrichment

events. The depletion event is related to widespread Archean crustal formation that left behind a refractory, harzburgitic residue. The high Mg-number and Ni and low Al_2O_3 and Na_2O in the lamproites relative to many other alkaline rocks, as well as the results of high P–T phase equilibrium studies are all consistent with the involvement of a harzburgitic mantle source in the genesis of the LHL. However, the high concentration of LILE and LREE in these lamproites indicates that the depletion event was followed by pervasive metasomatism. The negative Nb, Ti and Ta anomalies observed in the LHL trace element patterns indicate the involvement of subducted materials in metasomatizing the mantle source. The ancient age of this subduction-related metasomatism is supported by the Nd isotopic composition of the LHL (i.e. very low εNd values), and evidence from other igneous rocks emplaced in the Wyoming craton also indicates an ancient (>1 Ga) subduction event. As a result of the nature of the subducted materials and/or the high P–T conditions associated with the ancient subduction, the metasomatized mantle source developed moderate Rb/Sr, low U/Pb, and very low Sm/Nd time-integrated ratios. The enriched lithospheric mantle source subsequently behaved as a closed system until recent times (<100 Ma) when it was metasomatized by volatile-rich components derived from mantle upwelling, possibly related to the Yellowstone hotspot or plume, or more probably to *back-arc extension associated with subduction of the Farallon plate*. The newly added metasomatic components not only provided additional K_2O, volatiles and heat to the Wyoming sub-continental lithosphere but also lowered the solidus temperature to initiate partial melting in the source region.

ACKNOWLEDGEMENTS

We are grateful to A. Rukhlov, S. Farrell, D. Gold and E.A. Spencer, and especially B. Kjarsgaard, for constructive discussions and comments. I. de Jong is thanked for her assistance in the clean lab. Help by Bruce Taylor in obtaining oxygen isotopic data is much appreciated. Thanks go to M. Wilson, and the four reviewers, S. Bergman, T. Furman, J. Meen, and D. Prelevic, whose comments added greatly to this manuscript. This work was funded by an NSERC operating grant to K.B.

REFERENCES

Albers, M. & Christensen, R. R. (2001). Channeling of plume flow beneath mid-ocean ridges. *Earth and Planetary Science Letters* **187**, 207–220.

Anderson, D. L. (2005). Scoring hotspots: the plume and plate paradigms. In: Foulger, G. R., Natland, J. H., Presnall, D. C. & Anderson, D. L. (eds) *Plates, plumes, and paradigms. Geological Society of America, Special Paper* **388**, 31–54.

Artemieva, I. M. & Mooney, W. D. (2001). Thermal thickness and evolution of Precambrian lithosphere: a global study. *Journal of Geophysical Research, B, Solid Earth and Planets* **106**, 16387–16414.

Atkinson, W. J., Hughes, F. E. & Smith, C. B. (1984). A review of the kimberlitic rocks of Western Australia. In: Kornprobst, J. (ed.) *Kimberlites: I Kimberlites and Related Rocks 1*. Amsterdam: Elsevier, pp. 195–224.

Baker, M. B. & Stolper, E. M. (1994). The composition of high-pressure mantle melts: results from diamond aggregate experiments. *Mineralogical Magazine* **58**, 44–45.

Bell, K. & Simonetti, A. (1996). Carbonatite magmatism and plume activity: implications from Nd, Pb and Sr isotope systematics of Oldoinyo Lengai. *Journal of Petrology* **37**, 1321–1339.

Bell, K., Castorina, F., Rosatelli, G. & Stoppa, F. (2006). Plume activity, magmatism, and the geodynamic evolution of the central Mediterranean. *Annals of Geophysics* **49**, 357–371.

Bennet, V. C. & DePaolo, D. J. (1987). Proterozoic crustal history of the Western United States as determined by neodymium isotopic mapping. *Geological Society of America Bulletin* **99**, 674–685.

Bergman, S. C. (1987). Lamproites and other potassium-rich igneous rock, a review of their occurrences, mineralogy and geochemistry. In: Fitton, J. G. & Upton, B. G. J. (eds) *Alkaline Igneous Rocks. Geological Society, London, Special Publications* **30**, 103–189.

Bickford, M. E., Collerson, K. D., Lewry, J. F., Van Schmus, W. R. & Chiarenzelli, J. R. (1990). Proterozoic collisional tectonism in the Trans-Hudson Orogens, Saskatchewan. *Geology* **18**, 14–18.

Bird, P. (1984). Laramide crustal thickening event in the Rocky Mountain foreland and Great Plains. *Tectonics* **3**, 741–758.

Blackstone, D. L.,Jr (1983). Laramide compressional tectonics, southeastern Wyoming. *Contributions to Geology, University of Wyoming* **22**, 1–38.

Blackwell, D., David, D., Steele, J. & Carter, L. S. (1991). Heat-flow patterns of the North American continent: a discussion of the geothermal map of North America. In: Slemmons, D. B., Engdahl, E. R., Zoback, M. D. & Blackwell, D. D. (eds) *Neotectonics of North America. Boulder, CO: Geological Society of America* pp. 423–436.

Bradley, W. H. (1964). Geology of Green River Formation and Associated Eocene Rocks in Southwestern Wyoming and Adjacent Parts of Colorado and Utah. *US Geological Survey, Professional Papers* **496A**.

Camp, V. E. (1995). Mid-Miocene propagation of the Yellowstone mantle plume head beneath the Columbia River Basalt source region. *Geology* **23**, 435–438.

Carlson, R. W. & Irving, A. J. (1994). Depletion and enrichment history of subcontinental lithospheric mantle: an Os, Sr, Nd and Pb isotopic study of ultramafic xenoliths from the northwestern Wyoming Craton. *Earth and Planetary Science Letters* **126**, 457–472.

Carlson, R. W., Irving, A. J. & Hearn, B. C. (1999). Chemical and isotopic systematics of peridotite xenoliths from the Williams Kimberlite, Montana: clues to processes of lithosphere formation, modification and destruction. In: Gurney, J. J., Gurney, J. L., Pascoe, M. D. & Richardson, S. H. (eds) *Proceedings of the 7th International Kimberlite Conference*. Cape Town: Red Roof Design, pp. 90–98.

Carmichael, I. S. E. (1967). The mineralogy and petrology of the volcanic rocks from the Leucite Hills, Wyoming. *Contributions to Mineralogy and Petrology* **15**, 24–66.

Chamberlain, K. R., Frost, C. D. & Frost, B. R. (2003). Early Archean to Mesoproterozoic evolution of the Wyoming Province: Archean origins to modern lithospheric architecture. *Canadian Journal of Earth Sciences* **40**, 1357–1374.

Christiansen, R. L. (1993). The Yellowstone hot spot, deep mantle plume or upper mantle melting anomaly? *EOS Transactions, American Geophysical Union* **76**, 602.

Christiansen, R. L., Foulger, G. R. & Evans, J. R. (2002). Upper-mantle origin of the Yellowstone hotspot. *Geological Society of America Bulletin* **114**, 1245–1256.

Courtillot, V., Davaille, A., Besse, J. & Stock, J. (2003). Three distinct types of hotspots in the Earth's mantle. *Earth and Planetary Science Letters* **205**, 295–308.

Cox, K. G. (1988). The Karoo Province. In: MacDougall, J. D. (ed.) *Continental Flood Basalts*. Boston, MA: Kluwer Academic, pp. 239–271.

Cross, W. (1897). Igneous rocks of the Leucite Hills and Pilot Butte, Wyoming. *American Journal of Science* **4**, 115–141.

DePaolo, D. J. (1981). Trace element and isotopic effects of combined wallrock assimilation and fractional crystallization. *Earth and Planetary Science Letters* **53**, 189–202.

Downes, H., MacDonald, R., Upton, B. G. J., Cox, K. G., Bodinier, J., Mason, P. R. D., James, D. & Hill, P. G. (2004). Ultramafic xenoliths from the Bearpaw Mountains, Montana, USA: evidence for multiple metasomatic events in the lithospheric mantle beneath the Wyoming Craton. *Journal of Petrology* **45**, 1631–1662.

Dudás, F.Ö. (1991). Geochemistry of igneous rocks from the Crazy Mountains, Montana, and tectonic models for the Montana alkalic province. *Journal of Geophysical Research* **96**, 13261–13277.

Dudás, F.Ö., Carlson, R. W. & Eggler, D. H. (1987). Regional middle Proterozoic enrichment of the subcontinental mantle source of igneous rocks from central Montana. *Geology* **15**, 22–25.

Ebinger, C. J. & Sleep, N. H. (1998). Cenozoic magmatism throughout East Africa resulting from impact of a single plume. *Nature* **395**, 788–791.

Edgar, A. D. (1983). Relationships of ultrapotassic magmatism in the western U.S.A. to the Yellowstone plume. *Neues Jahrbuch für Mineralogie* **147**, 35–46.

Edgar, A. D. & Mitchell, R. H. (1997). Ultra high pressure–temperature melting experiments on an SiO_2-rich lamproite from Smokey Butte, Montana, derivation of siliceous lamproite magmas from enriched source deep in the continental mantle. *Journal of Petrology* **38**, 457–477.

Eggler, D. H., McCallum, M. E. & Kirkely, M. B. (1987). Kimberlite-transported nodules from Colorado-Wyoming: A record of enrichment of shallow portions of an infertile lithosphere. In: Morris, E. M. & Pasteris, J. D. (eds) *Mantle metasomatism and alkaline magmatism. Geological Society of America, Special Paper* **215**, 77–89.

Eggler, D. H., Meen, J. K., Welt, F., Dudás, F.Ö., Furlong, K. P., McCallum, M. E. & Carlson, R. W. (1988). Tectonomagmatism of the Wyoming Province. In: Drexler, J.W. & Larson, E. E. (eds) *Cenozoic Volcanism in the Southern Rocky mountains revisited: A tribute to Rudy C. Epis: Part 3. The Colorado School of Mines Quarterly,* **88**, 25–40.

Farmer, G. L., Bowring, S. A., Williams, M. L., Christensen, N. I., Matzel, J. & Stevens, L. (2005). Contrasting lower crustal evolution across an Archean–Proterozoic suture, physical, chemical and geochronologic studies of lower crustal xenoliths in southern Wyoming and northern Colorado. In: Keller, G.R. & Karlstrom, K.E. (eds) *The Rocky Mountain Region: an Evolving Lithosphere. Geophysical Monograph, American Geophysical Union* **154**, 139–162.

Feeley, T. C. (2003). Origin and tectonic implications of across-strike geochemical variations in the Eocene Absaroka volcanic province, United States. *Journal of Geology* **111**, 329–346.

Feeley, T. C. & Cosca, M. A. (2003). Time vs composition trends of magmatism at Sunlight volcano, Absaroka volcanic province, Wyoming. *Geological Society of America Bulletin* **115**, 714–728.

Feeley, T. C., Cosca, M. A. & Lindsay, C. R. (2002). Petrogenesis and implications of cryptic hybrid magmas from Washburn volcano, Absaroka volcanic province, USA. *Journal of Petrology* **43**, 663–703.

Fitton, J. G., James, D., Kempton, P. D., Ormerod, D. S. & Leeman, W. P. (1988). The role of lithospheric mantle in the generation of late Cenozoic basic magmas in the Western United States. *Journal of Petrology, Special Issue* 331–349.

Foley, S. F. (1992). Vein-plus-wall-rock melting mechanism in the lithosphere and the origin of potassic alkaline magmatism. *Lithos* **28**, 435–453.

Foley, S. F. (1993). An experimental study of olivine lamproite: first results from the diamond stability field. *Geochimica et Cosmochimica Acta* **57**, 483–489.

Foley, S. F., Taylor, W. R. & Green, D. H. (1986). The role of fluorine and oxygen fugacity in the genesis of the ultrapotassic rocks. *Contributions to Mineralogy and Petrology* **94**, 183–192.

Foley, S. F., Musselwhite, D. S. & van der Laan, S. R. (1999). Melt compositions from ultramafic vein assemblages in the lithospheric mantle: a comparison of cratonic and non-cratonic settings. In: Gurney, J. J., Gurney, J. L., Pascoe, M. D. & Richardson, S. H. (eds) *The J. B. Dawson Volume; Proceedings of the VIIth International Kimberlite Conference, Volume 1,* Cape Town, Red Roof Design, pp. 238–246.

Fraser, K. J. (1987). Petrogenesis of kimberlite from South Africa and lamproites from Western Australia and North America. Ph.D. thesis, The Open University, Milton Keynes, UK.

Frost, C. D., Frost, B. R., Chamberlain, K. R. & Hulsebosch, T. P. (1998). The late Archean history of the Wyoming Province as recorded by granitic magmatism in the Wind River Range, Wyoming. *Precambrian Research* **89**, 145–173.

Fukao, Y., Widiyantoro, S. & Obayashi, M. (2001). Stagnant slabs in the upper and lower mantle transition region. *Reviews of Geophysics* **39**, 291–323.

Haggerty, S. E. & Sautter, V. (1990). Ultradeep (greater than 300 kilometers), ultramafic upper mantle xenoliths. *Science* **248**, 993–996.

Harlan, S. S., Snee, L. W. & Geissman, J. W. (1996). $^{40}Ar/^{39}Ar$ geochronology and paleomagnetism of Independence volcano, Absaroka Volcanic Supergroup, Beartooth Mountains, Montana. *Canadian Journal of Earth Sciences* **33**, 1648–1654.

Hart, S. R. (1984). The DUPAL anomaly: a large-scale isotopic anomaly in the southern hemisphere. *Nature* **309**, 753–756.

Hawkesworth, C. J., Fraser, K. J. & Rogers, N. W. (1985). Kimberlites and lamproites, extreme products of mantle enrichment products. *Transactions of the Geological Society of South Africa* **88**, 439–447.

Hawkesworth, C. J., Kempton, P. D., Rogers, N. W., Ellam, R. M. & van Calsteren, P. W. (1990). Continental mantle lithosphere, and shallow level enrichment processes in the Earth's mantle. *Earth and Planetary Science Letters* **96**, 256–268.

Hergt, J. M., Peate, D. W. & Hawkesworth, C. J. (1991). The petrogenesis of Mesozoic Gondwana low-Ti flood basalts. *Earth and Planetary Science Letters* **105**, 134–148.

Herzberg, C., Raterron, P. & Zhang, J. (2000). New experimental observations on the anhydrous solidus for peridotite KLB-1. *Geochemistry, Geophysics, Geosystems* **1**(11) 2000GC000089.

Hildreth, W., Halliday, A. N. & Christiansen, R. L. (1991). Isotopic and chemical evidence concerning the genesis and contamination of basaltic and rhyolitic magma beneath the Yellowstone plateau volcanic field. *Journal of Petrology* **32**, 63–138.

Hirose, K. & Kushiro, I. (1993). Partial melting of dry peridotites at high pressures: determination of compositions of melts segregated from peridotite using aggregates of diamond. *Earth and Planetary Science Letters* **114**, 477–489.

Hoffman, P. F. (1989). Precambrian geology and tectonic history of North America. In: Bally, A. W. & Palmer, A. R. (eds) *The Geology of*

North America—an Overview. Boulder, CO: Geological Society of America, pp. 95–104.

Hofmann, A. W. (1997). Mantle geochemistry: the message from oceanic volcanism. *Nature* **385**, 219–229.

Ihinger, P. D., Watkins, J. M., Bernhardt, J. E. & Johnson, B. R. (2004). Yellowstone plumehead meets Farallon slab; a plausible mechanism driving North American continental tectonics for 80 My. *Geological Society of America, Abstracts with Programs* **36**, 95–96.

Jaques, A. L. & Milligan, P. R. (2004). Patterns and controls on the distribution of diamondiferous intrusions in Australia. *Lithos* **77**, 783–802.

Johnston, R. H. (1959). Geology of the Northern Leucite Hills, Sweetwater County, Wyoming. M.Sc. thesis, University of Wyoming, Laramie.

Kemp, J. F. & Knight, W. C. (1903). Leucite Hills of Wyoming. *Geological Society of America Bulletin* **14**, 305–336.

Konzett, J., Sweeney, R. J., Thompson, A. B. & Ulmer, P. (1997). Potassium amphibole stability in the upper mantle, an experimental study in a peralkaline KNCMASH system to 8·5 GPa. *Journal of Petrology* **38**, 537–568.

Kretz, R. (1983). Symbols for rock-forming minerals. *American Mineralogist* **68**, 277–279.

Kuehner, S. M. (1980). Petrogenesis of ultrapotassic rocks, Leucite Hills, Wyoming. M.Sc. thesis, University of Western Ontario, London, Ont.

Kuehner, S. M., Edgar, A. D. & Arima, M. (1981). Petrogenesis of the ultrapotassic rocks from the Leucite Hills, Wyoming. *American Mineralogist* **66**, 663–677.

Kushiro, I., Syono, Y. & Akimoto, S. (1967). Stability of phlogopite and possible presence of phlogopite in the Earth's upper mantle. *Earth and Planetary Science Letters* **3**, 197–203.

Lange, R. A., Carmichael, I. S. E. & Hall, C. M. (2000). $^{40}Ar/^{39}Ar$ chronology of the Leucite Hills, Wyoming: eruption rates, erosion rates, and an evolving temperature structure of the underlying mantle. *Earth and Planetary Science Letters* **174**, 329–340.

Leat, P. T., Thompson, R. N., Morrison, M. A., Hendry, G. L. & Dickin, A. P (1988). Compositionally diverse Miocene–Recent rift-related magmatism in NW Colorado: partial melting, and mixing of mafic magmas from three different asthenospheric and lithospheric mantle sources. *Journal of Petrology* **29**, 351–377.

Lee, C. A. (2005). Trace element evidence for hydrous metasomatism at the base of the North American lithosphere and possible association with Laramide low-angle subduction. *Journal of Geology* **113**, 673–685.

Le Maitre, R. W. (2002). *Igneous Rocks. A Classification and Glossary of Terms*. Cambridge: Cambridge University Press.

Lipman, P. W. (1980). Cenozoic volcanism in the western United States, implication for continental tectonics. In: Burchfiel, B. C., Oliver, J. E. & Silver, L. T. (eds) *Continental Tectonics*. Washington, DC: National Academy of Science, pp. 161–174.

Luth, R. W., Tronnes, R. G. & Cani, D. (1993). Volatile-bearing phases in the Earth's mantle. In: Luth, R. W. (ed.) *Short Course Handbook on Experiments at High Pressure and Applications to the Earth's Mantle. Mineralogical Association of Canada, Short Courses* **21**, 445–485.

MacDonald, R., Upton, B. G. J., Collerson, K. D., Hearn, B. C.,Jr & James, D. (1992). Potassic mafic lavas of the Bearpaw Mountains, Montana: mineralogy, chemistry, and origin. *Journal of Petrology* **33**, 305–346.

Madsen, J. K., Thorkelson, D. J., Friedman, R. M. & Marshall, D. D. (2006). Cenozoic to Recent plate configurations in the Pacific Basin; ridge subduction and slab window magmatism in western North America. *Geosphere* **2**, 11–34.

Marvin, C. F., Hearn, B. C., Mehnert, H. H., Naeser, C. W., Zartman, R. E. & Lindsay, D. A. (1980). Late Cretaceous–Paleocene–Eocene igneous activity in North–Central Montana. *Isochron West* **29**, 5–25.

Mattey, D. P., Lowry, D. & MacPherson, C. (1994). Oxygen isotope composition of upper mantle peridotites. *Earth and Planetary Science Letters* **128**, 231–241.

McCulloch, M. T., Jaques, A. L., Nelson, D. R. & Lewis, J. D. (1983). Nd and Sr isotopes in kimberlites and lamproites from Western Australia: an enriched mantle origin. *Nature* **302**, 400–403.

McDonough, W. F. & Sun, S. S. (1995). Composition of the Earth. *Chemical Geology* **120**, 223–253.

Mcdowell, F. W. (1971). K–Ar ages of igneous rocks from the western United States. *Isochron West* **2**, 1–16.

McKenzie, D. (1989). Some remarks on the movement of small melt fractions in the mantle. *Earth and Planetary Science Letters* **95**, 53–72.

Meen, J. K. & Eggler, D. H. (1987). Petrology and geochemistry of the Cretaceous Independence volcanic suite, Absaroka Mountains, Montana: clues to the composition of the Archean sub-Montanan mantle. *Geological Society of America Bulletin* **98**, 238–247.

Meen, J. K., Ayers, J. C. & Fregeau, E. J. (1989). A model of mantle metasomatism by carbonated alkaline melts: trace-element and isotopic compositions of mantle source regions of carbonatite and other continental igneous rocks. In: Bell, K. (ed.) *Carbonatites: Genesis and Evolution. Unwin Hyman, London*. pp. 464–499.

Menzies, M. A. (1987). Alkaline rocks and their inclusions, a window on the Earth's interior. In: Fitton, J. G. & Upton, B. G. J. (eds) *Alkaline Igneous Rocks. Geological Society, London, Special Publications* **30**, 15–27.

Menzies, M. A. & Hawkesworth, C. J. (1987). *Mantle Metasomatism*. London: Academic Press.

Menzies, M. A. & Wass, S. Y. (1983). CO_2- and LREE-rich mantle below eastern Australia: a REE and isotopic study of alkaline magmas and apatite-rich mantle xenoliths from the Southern Highlands province, Australia. *Earth and Planetary Science Letters* **65**, 287–302.

Mirnejad, H. (2002). Isotope geochemistry, petrology, and source evaluation of the Leucite Hills lamproites, Wyoming. Ph.D. thesis, Carleton University, Ottawa, Ont.

Mitchell, R. H. (1985). A review of the mineralogy of lamproites. *Transactions of the Geological Society of South Africa* **88**, 411–437.

Mitchell, R. H. (1989). Aspects of the petrology of kimberlites and lamproites: some definitions and distinctions. In: Ross, J., Jaques, A. L., Ferguson, J., Green, D. H., O'Reilly, S. Y., Danchin, R. V. & Janse, A. J. A. (eds) *Kimberlites and Related Rocks. Special Publications, Geological Society of Australia,* **14**, 1–45.

Mitchell, R. H. (1995a). Melting experiments on a sanidine phlogopite lamproite at 4–7 GPa and their bearing on the source of lamproitic magmas. *Journal of Petrology* **36**, 1455–1474.

Mitchell, R. H. (1995b). *Kimberlites, Orangeites and Related Rocks*. New York: Plenum.

Mitchell, R. H. & Bergman, S. C. (1991). *Petrology of Lamproites*. New York: Plenum.

Mitchell, R. H. & Edgar, A. D. (2002). Melting experiments on SiO_2-rich lamproites to 6·4 GPa and their bearing on the sources of lamproite magmas. *Mineralogy and Petrology* **74**, 115–128.

Mitchell, R. H., Platt, R G. & Downey, M (1987). Petrology of lamproites from Smoky Butte, Montana. *Journal of Petrology* **28**, 645–677.

Moore, R. O. & Gurney, J. J. (1991). Pyroxene solid solution in garnets included in diamond. *Nature* **318**, 553–555.

Mueller, P. A. & Wooden, J. L. (1988). Evidence for Archean subduction and crustal recycling, Wyoming province. *Geology* **16**, 871–874.

Mueller, P. A., Wooden, J. L., Schulz, K. & Bowes, D. R. (1983). Incompatible element-rich andesitic amphibolites from the Archean of Montana and Wyoming: evidence for mantle metasomatism. *Geology* **11**, 203–2060.

Murphy, D. T., Collerson, K. D. & Kamber, B. S. (2002). Lamproites from Gaussberg, Antarctica, possible transition zone melts of Archean subducted sediments. *Journal of Petrology* **43**, 981–1001.

Murphy, J. B., Hynes, A. J., Johnston, S. T. & Keppie, J. D. (2003). Reconstructing the ancestral Yellowstone plume from accreted seamounts and its relationship to flat-slab subduction. *Tectonophysics* **365**, 185–194.

Nelson, D. R. (1992). Isotopic characteristics of potassic rocks—evidence for the involvement of subducted sediments in magma genesis. *Lithos* **25**, 403–420.

Nelson, D. R. & McCulloch, M. T. (1989). Enriched mantle components and mantle recycling of sediments. In: Ross, J., Jaques, A. L., Ferguson, J., Green, D. H., O'Reilly, S. Y., Danchin, R. V. & Janse, A. J. A. (eds) *Kimberlites and Related Rocks. Special Publications, Geological Society of Australia* **14**, 560–570.

Nixon, P. H., Thirlwall, M. F., Buckley, F. & Davies, C. J. (1984) Spanish and Western Australia lamproites; aspects of whole rock geochemistry. In: Kornprobst, J.(ed) *Kimberlites: I, Kimberlites and related rocks. Elsevier Sci. Publ., Amsterdam, Netherlands* pp. 285–296.

O'Brien, H. E., Irving, A. J. & McCallum, I. S. (1991). Eocene potassic magmatism in the Highwood Mountains, Montana; petrology, geochemistry, and tectonic implications. *Journal of Geophysical Research* **96**, 13237–13260.

O'Brien, H. E., Irving, A. J., McCallum, I. S. & Thirwall, M. F. (1995). Sr, Nd and Pb isotopic evidence for the interaction of post-subduction asthenospheric potassic mafic magmas of the Highwood Montana, Montana, USA, with ancient Wyoming craton lithospheric mantle. *Geochimica et Cosmochima Acta* **59**, 4539–4556.

Ogden, P. R. (1979). The geology, major element geochemistry and petrogenesis of the Leucite Hills volcanic rocks, Wyoming. PhD thesis, University of Wyoming, Laramie.

Othman, D. B., White, W. M. & Patchett, J. (1989). The geochemistry of marine sediments, island arc magma genesis, and crust–mantle recycling. *Earth and Planetary Science Letters* **94**, 1–21.

Pearce, J. (1982). Trace element characteristics of lavas from destructive plate boundaries. In: Thorpe, R. S. (ed.) *Andesites, Orogenic Andesites and Related Rocks*. Chichester: John Wiley, pp. 525–548.

Peccerillo, A. & Lustrino, M. (2005). Compositional variations of Plio-Quaternary magmatism in the circum-Tyrrhenian area: deep versus shallow mantle processes. In: Foulger, G. R., Natland, J. H., Presnall, D. C. & Anderson, D. L. (eds) *Plates, plumes, and paradigms. Geological Society of America, Special Paper* **388**, 421–434.

Peterman, Z. E., Hedge, C. E. & Braddock, W. A. (1968). Age of Precambrian events in the northeast Front Range, Colorado. *Journal of Geophysical Research* **73**, 2277–2296.

Plank, T. & Langmuir, C. H. (1998). The chemical composition of subducted sediment and its consequences for the crust and mantle. *Chemical Geology* **145**, 325–394.

Ringwood, A. E., Kesson, S. E., Hibberson, W. & Ware, N. (1992). Origin of kimberlites and related magmas. *Earth and Planetary Science Letters* **113**, 521–538.

Rudnick, R. L., Ireland, T. R., Gehrels, G., Irving, A. J., Chesley, J. T. & Hanchar, J. M. (1999). Dating mantle metasomatism; U–Pb geochronology of zircons in cratonic mantle xenoliths from Montana and Tanzania. In: Gurney, J. J., Gurney, J. L., Pascoe, M. D. & Richardson, S. H. (eds) *Proceedings of the 7th International Kimberlite Conference*. Cape Town: Red Roof Design, pp. 728–735.

Salters, V. J. M. & Longhi, J. (1999). Trace element partitioning during the initial stages of melting beneath mid-ocean ridges. *Earth and Planetary Science Letters* **166**, 15–30.

Sato, K., Satsura, T. & Ito, E. (1997). Phase relations of natural phlogopite with and without enstatite up to 8 GPa: implications for mantle metasomatism. *Earth and Planetary Science Letters* **146**, 511–526.

Scambos, T. A. (1987). Sr and Nd isotope ratios for the Missouri Breaks diatreme, central Montana. *Geological Society of America, Abstracts with Programs* **19**, 830–831.

Schmidt, K. H., Bottazzi, P., Vannucci, R. & Mengel, K. (1999). Trace element partitioning between phlogopite, clinopyroxene and leucite lamproite melt. *Earth and Planetary Science Letters* **168**, 287–299.

Schutt, D., Eugene, D., Humphreys, E. D. & Dueker, K. (1998). Anisotropy of the Yellowstone Hot Spot wake, eastern Snake River plain, Idaho. In: Plomerova, J, Liebermann, R. C. & Babuska, V. (eds) *Geodynamics of lithosphere and Earth's mantle: seismic anisotropy as a record of the past and present dynamic processes. Source Pure and Applied Geophysics, Speical Issue* **151**(2–4), 443–462.

Scott Smith, B. H. & Skinner, E. M. W. (1984a). Diamondiferous lamproites. *Journal of Geology* **92**, 433–438.

Scott Smith, B. H. & Skinner, E. M. W. (1984b). A new look at Prairie Creek, Arkansas. In: Kornprobst, J. (ed.) *Proceedings of the Third International Kimberlite Conference, 1*. Amsterdam: Elsevier, pp. 255–284.

Severinghaus, J. & Atwater, T. (1990). Cenozoic geometry and thermal state of the subducting slabs beneath North America. In: Wernicke, B. P. (ed) *Basin and Range Extensional Tectonics near the Latitude of Las Vegas, Nevada. Geological Society of America, Memoirs* **176**, 1–22.

Simons, F. J., Zielhuis, A. & Van der Hilst, R. D. (1999). The deep structure of the Australian continent from surface wave tomography. *Lithos* **48**, 17–43.

Skinner, E. M. W. (1989). Contrasting group I and II kimberlite petrology: towards a genetic model for kimberlites. In: Ross, J,, Jaques, A. L., Ferguson, J., Green, D. H., O'Reilly, S. Y., Danchin, R. V. & Janse, A. J. A. (eds) *Kimberlites and Related Rocks. Special Publications, Geological Society of Australia,* **14**, 528–544.

Smith, C. B. (1983). Pb, Sr and Nd isotopic evidence for sources of southern African Cretaceous kimberlites. *Nature* **304**, 51–54.

Smith, R. B. & Braile, L. W. (1994). The Yellowstone hotspot. *Journal of Volcanology and Geothermal Research* **61**, 121–187.

Smith, R. B. & Siegel, L. J. (2000). Windows into the Earth: the Geologic Story of Yellowstone and Grand Teton National Parks. Oxford: Oxford University Press.

Smithson, S. B. (1959). The geology of the southeastern Leucite Hill, Sweetwater County, Wyoming. M.Sc. thesis, University of Wyoming, Laramie.

Stacey, J. S. & Kramers, J. D. (1975). Approximation of terrestrial lead isotope evolution by a two-stage model. *Earth and Planetary Science Letters* **26**, 207–221.

Stuckless, J. S., Hedge, C. E., Worl, R. G., Simmons, K. R., Nkomo, I. T. & Wenner, D. B. (1985). Isotopic studies of the late Archean plutonic rocks of the Wind River Range, Wyoming. *Geological Society of America Bulletin* **96**, 850–860.

Tainton, K. M. & McKenzie, D. (1994). The generation of kimberlites, lamproites and their source rocks. *Journal of Petrology* **35**, 787–817.

Tronnes, R. G., Takahashi, E. & Scarfe, C. M. (1988). Stability of K-richterite and phlogopite to 14 GPa. *EOS Transactions, American Geophysical Union* **69**, 1510–1511.

Turner, S. P., Platt, J. P., George, R. M., Kelley, S. P., Pearson, D. G. & Nowell, G. M. (1999). Magmatism associated with orogenic

collapse of the Betic–Alboran Domain, SE Spain. *Journal of Petrology* **40**, 1011–1036.

Vollmer, R., Ogden, P., Schilling, J. G., Kingsley, R. H. & Waggoner, D. G. (1984). Nd and Sr isotopes in ultrapotassic volcanic rocks from the Leucite Hills, Wyoming. *Contributions to Mineralogy and Petrology* **87**, 359–368.

Walker, K. T., Bokelmann, G. H. R. & Klemperer, S. L. (2004). Shear-wave splitting beneath the Snake River plain suggests a mantle upwelling beneath eastern Nevada, USA. *Earth and Planetary Science Letters* **222**, 529–542.

Wang, K., Plank, T., Walker, J. D. & Smith, E. I. (2002). A mantle melting profile across the Basin and Range, SW USA. *Journal of Geophysical Research B, Solid Earth and Planets* **107**, 21 pp.

Wasylenki, L. E., Baker, M. B., Hirschmann, M. M. & Stolper, E. M. (1996). The effect of source depletion on equilibrium mantle melting. *EOS Transactions, American Geophysical Union* **77**(46), F847.

Wedepohl, K. H. (1995). The composition of the continental crust. *Geochimica et Cosmochimca Acta* **59**, 1217–1232.

Wheller, G. E., Varne, R., Foden, J. D. & Abbot, M. J. (1987). Geochemistry of Quaternary volcanism in the Sunda–Bana arc, Indonesia, and three-component genesis of island-arc basaltic magmas. *Journal of Volcanology and Geothermal Research* **32**, 137–160.

White, W. M. & Dupré, B. (1986). Sediment subduction and magma genesis in the Lesser Antilles: isotopic and trace element constraints. *Journal of Geophysical Research* **91**, 5927–5941.

White, R. & McKenzie, D. (1989). Magmatism at rift zones: the generation of volcanic continental margins and flood basalts. *Journal of Geophysical Research, B, Solid Earth and Planets* **94**, 7685–7729.

White, S. H., de, B, oorder, H. & Smith, C. B. (1995). Structural controls of kimberlite and lamproite emplacement. *Journal of Geochemical Exploration* **53**, 245–264.

Wilson, M. (1989). *Igneous Petrogenesis: a Global Tectonic Approach*. London: Chapman & Hall.

Wooden, J. L. & Mueller, P. A. (1988). Pb, Sr and Nd isotopic compositions of a suite of Late Archean igneous rocks, eastern Beartooth Mountains: implications for crust–mantle evolution. *Earth and Planetary Science Letters* **87**, 59–72.

Woolley, A. R., Edgar, A. D., Le Bas, M. J., Mitchell, R. H., Rock, N. M. S. & Scott Smith, B. H. (1996). Classification of lamprophyres, lamproites, kimberlites, and the kalsilitic, melilitic, and leucitic rocks. *Canadian Mineralogist* **34**, 175–186.

Xue, M. & Allen, R. M. (2005). Asthenospheric channeling of the Icelandic upwelling: evidence from seismic anisotropy. *Earth and Planetary Science Letters* **235**, 167–182.

Zirkel, F. (1867). Microscopical petrography. *US Geology Exploration 40th Parallel Report* **6**, 259–261.

Zoback, M. L., McKee, E. H., Blakely, R. J. & Thompson, G. A. (1994). The northern Nevada Rift: regional tectono-magmatic relations and middle-Miocene stress direction. *Geological Society of America Bulletin* **106**, 371–382.